«ФИЗИКА ЭЛЕМЕНТАРНЫХ ЧАСТИЦ И АТОМНОГО ЯДРА»
2000, ТОМ 31, ВЫП. 3

539.12.01

THERMODYNAMICS OF A CHIRAL EFFECTIVE MODEL WITH AXIAL AND TRACE ANOMALIES

B. Van den Bossche

Université de Liège, Institut de Physique B5, Sart Tilman, B-4000 Liège 1, Belgium

«ФИЗИКА ЭЛЕМЕНТАРНЫХ ЧАСТИЦ И АТОМНОГО ЯДРА»
2000, ТОМ 31, ВЫП. 3

УДК 539.12.01

THERMODYNAMICS OF A CHIRAL EFFECTIVE MODEL WITH AXIAL AND TRACE ANOMALIES

B. Van den Bossche

Université de Liège, Institut de Physique B5, Sart Tilman, B-4000 Liège 1, Belgium

The Nambu–Jona-Lasinio (NJL) model with scale and axial $U_A(1)$ anomalies is introduced at finite temperature and density in the case of three flavors (u, d, s). It is then used to evaluate condensates and thermodynamical functions (pressure, energy and entropy densities). We mainly focus on analytical results.

Вводится модель Намбу–Иона-Лазинио (НИЛ) с масштабной и аксиальной $U_A(1)$ аномалиями при конечной температуре и плотности в случае трех ароматов (u, d, s). Затем она используется для вычисления конденсатов и термодинамических функций (давления, плотности энергии и энтропии). В основном представлены аналитические результаты.

1. INTRODUCTION

Quantum chromodynamics, the fundamental theory of strong interaction, is defined through the Lagrangian [1]

$$\mathcal{L}_{QCD} = \bar{q}(i\gamma^\mu\partial_\mu - m)q - \frac{1}{4}(F^a_{\mu\nu})^2 + g\bar{q}\gamma^\mu A_\mu q, \tag{1}$$

where q is the quark field in flavor and color spaces (in the fundamental representation) and g is the coupling constant. The quantity A_μ is a shortened notation for the eight gluon fields ($A_\mu = A^a_\mu\lambda^a/2$) in the adjoint representation. They come into the Yang–Mills Lagrangian in the combination

$$F^a_{\mu\nu} = \partial_\mu A^a_\nu - \partial_\nu A^a_\mu + g f^{abc} A^b_\mu A^c_\nu, \tag{2}$$

which gives rise to an interaction term between gluons (three- and four-gluon couplings), due to the non-Abelian structure of the theory. (The totally antisymmetrical coefficients f^{abc} are the structure constants of $SU(3)$.) This interaction, with the fact that the coupling constant is high at low energy, prevents making a perturbative analysis to describe hadronic matter. The understanding of this physics requires putting QCD on a lattice or making use of effective model, the latter being supposed to mimic the true theory in a given range of energy–momentum. In the low energy regime, chiral symmetry is believed to play the

key role. In the following, we shall use a model which implement this symmetry: the Nambu–Jona-Lasinio or NJL model. This model was introduced some time ago in the nucleon language [2, 3]. With quark degrees of freedom, it has regain new interest after the work of Volkov [4]. For three flavors in the scalar and pseudoscalar sectors, it is described by the Lagrangian

$$\mathcal{L}_{NJL} = \bar{q}(i\partial\!\!\!/ - m)q + G_S \sum_{i=0}^{8} [(\bar{q}\frac{(\lambda^i)_F}{2}q)^2 + (\bar{q}i\gamma_5\frac{(\lambda^i)_F}{2}q)^2]. \qquad (3)$$

Although having short-comings such as the lack of renormalizability and of confinement, the model has the attractive features of being relativistically invariant and respecting some of the symmetries of QCD (among them chiral symmetry, in the case of vanishing quark masses) while being mathematically tractable due to the locality property of the 4-quark interaction.

The NJL model has already been extensively studied by several groups. We can only mention a few, our purpose being here to describe the scaled version of the model*. A recent work has been done by Ripka** [6] in a book which contains an in-depth analysis of regularization procedures and symmetry conserving approximations; Klevansky [7] and Hatsuda and Kunihiro [8] give a general introduction to NJL, both in the vacuum and at finite temperature and density; Alkofer, Reinhardt and Weigel [9] mainly applied the model to discuss baryons as chiral solitons, as also done by Goeke and collaborators [10]; Bijnens [11] discusses chiral perturbation theory within NJL; Alkofer, Ebert, Reinhardt and Volkov [12, 13] hadronize the NJL model (both mesons and baryons); Vogl and Weise [14] and Weise [15] review several of the above-mentioned topics: bosonization and hadronization, finite density and temperature effects. Finally, a scaled NJL model in the same spirit as the one introduced here has been investigated in [16–18].

In the following, we shall study a modification of the Lagrangian (3) which takes into account the scale and axial anomalies of QCD. The motivation to proceed in this way is the following: the NJL model is taken into account because it is believed that its (global) symmetries, that it shares with QCD, are a key concept to understand the underlying strong theory. Being based on argument symmetry, it seems then natural to supply the model with other symmetry related physics: the anomaly one. Anomalies are symmetries of the classical action which are no more symmetries of the quantum world. Replacing the QCD Lagrangian by the NJL one, we have thrown away the scale and (strong) axial anomalies. Since the NJL model is intended to be used mainly at the mean field level, these

*For more references (but still a nonexhaustive list), see [5].

**This book is not restricted to the NJL model.

anomalies are introduced by hand by adding effective terms. In this way, quantum effects can be taken into account at the level of a tree effective theory.

Following [19], we give first a resume of the symmetries relevant to QCD and NJL, for three flavors of quark u, d, s.

A. Symmetries. In the following, we take the convention to denote by m the current quark mass matrix $\mathrm{diag}(m_u, m_d, m_s)$, and by q the vector representing quarks in the flavor space $q = \mathrm{diag}(q_u, q_d, q_s)$. The indicated transformations leave the action invariant under certain circumstances that we specify.

• **Global gauge symmetry**: NJL is globally color invariant: color enters only through the number N_c of each quark flavor.

• **Scale symmetry**:

$$\begin{cases} x_\mu \to \lambda^{-1} x_\mu, \\ A^a_\mu \to \lambda A^a_\mu, \\ q \to \lambda^{3/2} q, \end{cases}$$

is exact, at the level of the classical action, in the limit of vanishing current quark mass $m = 0$. However, this symmetry is broken by quantum effects.

• **Vector $U(1)_V$ symmetry or Baryonic number conservation**: $q \to \exp(i\alpha)q$.

• **Quark number conservation**: $q_i \to \exp(i\alpha_i)q_i$ $(i = u, d, s)$: each flavor has its own conserved number.

• **Axial $U(1)_A$ symmetry**: $q \to \exp(i\gamma_5\alpha)q$ is exact, at the level of the classical Lagrangian, in the limit of vanishing current quark mass $m = 0$. This symmetry is broken by quantum effects, which explains why it is not seen in the spectrum of physical states.

• **Isospin symmetry**:

$$q \equiv \begin{pmatrix} u \\ d \end{pmatrix} \to \exp(i\tau^a \alpha_a) q \ , \quad a = 1, ..., 3.$$

Isospin symmetry is exact in the limit where light quark masses are equal $m_u = m_d$ (τ_a are the Pauli matrices).

• **Vector $SU(3)_V$ symmetry**:

$$q \equiv \begin{pmatrix} u \\ d \\ s \end{pmatrix} \to \exp(i\frac{\lambda_a}{2}\alpha^a_V) q \ , \quad a = 1, ..., 8.$$

Isospin symmetry can be generalized to the three-flavor case and explains why the hadrons are approximately ordered into multiplets.

• **Axial $SU(2)_A$ and $SU(3)_A$ symmetries**:

$$q \equiv \begin{pmatrix} u \\ d \\ s \end{pmatrix} \to \exp(i\gamma_5\frac{\lambda_a}{2}\alpha^a_A) q \ , \quad a = 1, ..., 8 \quad (SU(2)_A : \lambda_a \to \tau_a).$$

This symmetry is exact as long as $m_u = m_d = m_s = 0$. It is however not seen in the spectrum. Since axial transformations alter the parity that is associated with a state, a manifestation of $SU(2,3)_A$ in nature would require that each isospin (or $SU(3)_V$) multiplet be accompanied by a mirror multiplet of opposite parity. In the same way, since we do not observe opposite parity partners to all hadrons, the $U(1)_A$ symmetry cannot be realized directly by QCD. While the axial $SU(3)_A$ symmetry is realized in the Goldstone mode through the dynamical breaking of chiral symmetry, $U(1)_A$ is never realized, being completely broken by quantum effects (the anomaly).

• **Chiral symmetry**: vector and axial $SU(3)$ symmetries can be combined to realize transformations on the left and right parts of the quarks ($q_{\substack{R\\L}} \equiv \frac{1 \mp \gamma_5}{2} q$):

$$SU(3)_V \otimes SU(3)_A \leftrightarrow SU(3)_L \otimes SU(3)_R,$$

where

$$SU(3)_L \Rightarrow q_L \rightarrow \exp(i\frac{\lambda_a}{2}\alpha_L^a) q_L,\ SU(3)_R \Rightarrow q_R \rightarrow \exp(i\frac{\lambda_a}{2}\alpha_R^a) q_R.$$

Under chiral symmetry, left-handed and right-handed quarks transform independently. This symmetry is broken by the quark mass matrix m. Apart from this explicit breaking, chiral symmetry is also spontaneously broken down to $SU(3)_V$.

As mentioned above, a symmetry can be manifested in several ways.

• It may remain exact.

• It may be explicitly broken (this is the case of isospin symmetry in the limit $m_u \neq m_d$).

• It may be hidden. It is an invariance of the action but not of the ground state: the symmetry is not seen in the spectrum of physical states. Two types of mechanisms [19] are possible: the symmetry can be spontaneously broken (such as the $SU(2)_L$ symmetry in electroweak interactions), or dynamically broken (due to self interactions of the considered fields) as for chiral $SU(2,3)_L \otimes SU(2,3)_R$ symmetry in QCD. In the latter case, there exists a composite order parameter which, in the case of dynamical chiral symmetry breaking, is often chosen as the quark condensate, although other order parameters are possible.

In the following, we shall use the term «spontaneous symmetry breaking» to describe both cases of hidden symmetry, making the distinction when appropriate.

The Goldstone theorem is intimately related to the notion of hidden symmetry and states that if a theory has a continuous symmetry of the Lagrangian which is not a symmetry of the vacuum, there must exist one or more massless (Goldstone) bosons. Goldstone theorem and the dynamical breaking of chiral symmetry explain the small pseudoscalar nonet mass ($\pi_0, \pi_\pm, K_0, \bar{K}_0, \eta, \eta'$), but for the η' which is too heavy.

The breaking of chiral symmetry can be summarized by

$$SU(3)_L \otimes SU(3)_R \Rightarrow SU(3)_V .$$

• The symmetry may have an anomaly, as for the axial $U(1)_A$ and scale symmetries of QCD. Even if the quark masses are vanishing, the divergence of the corresponding current is nonvanishing. For the axial $U(1)$ symmetry, we get ($\tilde{F}$ is the dual of F, $\beta_{\rm QCD}$ is the Callan–Symanzik β-function of QCD and γ_m is the mass anomalous dimension)

$$\partial^\mu(\bar{q}\gamma_\mu\gamma_5\frac{\lambda^0}{2}q) = 2i\bar{q}\gamma_5 m^0\frac{\lambda^0}{2}q + \sqrt{\frac{3}{2}}\frac{g^2}{32\pi^2}F^a_{\mu\nu}\tilde{F}^{\mu\nu}_a, \tag{4}$$

while the scale anomaly leads to

$$\partial_\mu J^\mu = \theta^\mu_\mu = (1+\gamma_m)\sum_{i=1}^{N_F}\bar{q}_i m_i q_i + \frac{\beta_{\rm QCD}}{2g}F^a_{\mu\nu}F^{\mu\nu}_a. \tag{5}$$

The strong axial anomaly (4) is believed to give its high mass to the η' particle compared to the other members of the pseudoscalar nonet.

B. Effective Action. The Lagrangian (3) is used at tree level. If we want this order to implement the full quantum aspects of QCD, it is necessary to supplement it with a term which, while still invariant under the true symmetries of QCD, has to break the axial $U(1)_A$ and scale invariances. Axial $U(1)_A$ anomaly can be related to the formation of instantons [20–22] and yields anomalous contributions to the η and η' masses. A 't Hooft determinant is often taken to mimic the anomaly, althought other forms can be chosen (see [20, 21, 23–26]). We shall use here the simplest approach, consisting in just adding a mass term $a^2\xi\eta_0^2$ (see Eq. (11)) for the pseudoscalar singlet η_0 particle, with ξ the parameter modelizing the anomaly.

Figure 1 shows the modification of the η and η' mass when the ξ parameter is varied. It is clear that, removing it, the η has the same mass as the pion, while the η' is similar, but with the strange quark instead of the up.

As for the axial anomaly, the effect of the trace anomaly has to be added by hand.

Several steps are necessary in order to construct the modified NJL model in the perspective of the symmetries and anomalies as described above. In view of the way of treating the axial anomaly (mass term for the η_0), it is better to work on the bosonized version of the model* which leads to the partition function

$$\mathcal{Z}_{NJL} = \int \mathcal{D}\varphi^a \exp\left(-I_{\rm eff}\right), \tag{6}$$

*Hadronization techniques are reviewed in [27, 28] and [12, 13].

with* [29–31]

$$I_{\rm eff} \;=\; -{\rm Tr}\ln(-i\partial\!\!\!/ + m^0 - W\!\!\!/ + \varphi^a\Gamma^a) + \int d^4x \frac{a^2}{2}(\varphi^a)^2, \tag{7}$$

$$\varphi_a \;=\; (\sigma_a, \pi_a),\ a = 0, ..., 8 \quad (\pi_0 \equiv \eta_0, \pi_8 \equiv \eta_8), \tag{8}$$

$$\Gamma_a \;=\; (\lambda_a, i\gamma_5\lambda_5),\ a = 0, ..., 8, \tag{9}$$

$${\rm Tr}O \;=\; {\rm tr}\int d^4x\,\langle x|O|x\rangle \ , \qquad \int d^4x = \int_0^\beta d\tau \int_\Omega d^3x, \tag{10}$$

where ${\rm tr}$ is the trace w.r.t. internal d.o.f. (Dirac, color, flavor), $\beta = 1/T$ is the inverse temperature, $W_\nu = (-i{\rm diag}(\mu_u, \mu_d, \mu_s), 0, 0, 0)$ and Ω is the volume of the system.

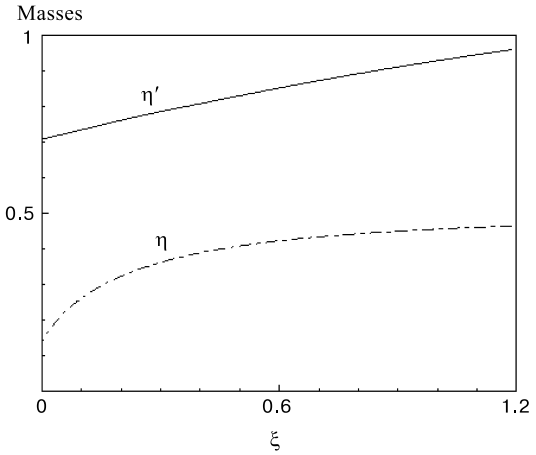

Fig. 1. $\eta,\ \eta'$ mass variation as a function of the ξ axial anomaly parameter

As mentioned above, the axial anomaly is introduced through a mass term for the η_0 particle. The scale invariance and anomaly, on the other hand, can be included in the effective action in a similar way, through the introduction of a dilaton field χ of scale dimension 1 (see for example [32, 33]). For details and more references, the reader is referred to [5, 34]. Although it is questionable [35] to use the dilaton field as an order parameter associated with gluon confinement,

*The Euclidean space is used from now on.

we shall adopt this point of view as in the works [36, 37]. Finally, the effective action defining the scaled NJL model is

$$I_{\rm eff} = -{\rm Tr}_{\Lambda\chi}\ln(-i\partial\!\!\!/ + m^0 + \varphi_a\Gamma_a - V\!\!\!/) + \int d^4x \frac{a^2}{2}\chi^2\varphi_a^2 + \int d^4x\left\{\frac{a^2}{2}\xi\chi^2\pi_0^2 + \frac{1}{2}(\partial_\mu\chi)^2 + \frac{b^2}{16}\left(\chi^4\ln(\frac{\chi^4}{\chi_G^4}) - (\chi^4 - \chi_G^4)\right)\right\}, \quad (11)$$

which takes into account axial and scale anomalies, and where a cut-off Λ has been included in the functional trace in order to take into account the lack of renormalizability*.

The main contribution to the partition function comes from the point which minimizes the effective action. Mathematically, this corresponds to finding the saddle point approximation to the path integral while, physically, it corresponds to a maximization of the pressure. In the present model, such an extremality condition leads to gap equations (or Dyson–Schwinger equations) for the constituent quark masses similar to that of the usual NJL model, but for a χ dependence:

$$a^2\chi_s^2\,(M_u - m_u) = 8N_cM_ug_{M_u,\beta,\mu_u}, \quad (12)$$

$$a^2\chi_s^2\,(M_s - m_s) = 8N_cM_sg_{M_s,\beta,\mu_s}, \quad (13)$$

with

$$g_{M_i,\beta,\mu_i} = \frac{1}{\beta\Omega}\sum_k \frac{1}{k_i^{*2} + {M_i}^2}, \quad i = u, s,$$

and $k_i^* = (k_0 - i\mu_i, \vec{k}), k_0 = (2n+1)\pi\beta$, the odd Matsubara frequencies being related to the anti-commutating nature of the fermions.

Moreover, there is a new equation, corresponding to the extremality condition for the dilaton field (this latter equation also contains the constituent quark masses):

*The cut-off breaks scale invariance. Supplementing it with a dilaton field, as described in [38], allows to restore it.

$$\exp\left\{-\frac{a^2}{2\chi_0^2}\left[{M_u^0}^2\left(1-\frac{m_u}{M_u^0}\right)^2+\frac{{M_s^0}^2}{2}\left(1-\frac{m_s}{M_s^0}\right)^2\right]\right\}$$
$$\times\frac{\left[(\Lambda\chi_0)^2+{M_u^0}^2\right]^{\frac{2N_c\Lambda^4}{8\pi^2}}}{{\chi_0}^{b^2/2}}\left[(\Lambda\chi_0)^2+{M_s^0}^2\right]^{\frac{N_c\Lambda^4}{8\pi^2}}$$
$$=\exp\left\{-\frac{a^2}{2{\chi_s}^2}\left[M_u^2\left(1-\frac{m_u}{M_u}\right)^2+\frac{M_s^2}{2}\left(1-\frac{m_s}{M_s}\right)^2\right]\right\}$$
$$\times\frac{\left[(\Lambda\chi_s)^2+{M_u}^2\right]^{\frac{2N_c\Lambda^4}{8\pi^2}}}{{\chi_s}^{b^2/2}}\left[(\Lambda\chi_s)^2+{M_s}^2\right]^{\frac{N_c\Lambda^4}{8\pi^2}}. \tag{14}$$

In the 2-degenerate flavor case, we then have two coupled equations: one is the gap Equation (12), while the other is (14) without the strange content. Since they are nonlinear, we can expect different results compared to a pure NJL model. And indeed, we have different results: according to the set of parameters, we can have a second or first order phase transition (restoration of chiral symmetry) w.r.t. the temperature, at zero density. The usual NJL model only allows a second order phase transition. When a third quark with a different mass is added, such as the strange quark, we have one more gap equation and the behaviour can be even more complicated: noncoincident second order phase transition for both quarks, or coincident first order, or noncoincident first order, or a first transition for one species while the other feels a second order phase transition. It is clear that in such a complicated situation, working with the gap equations, coming from a derivative condition, can be a very hard task and it is useful to turn to a global condition, looking directly at the great potential (or the pressure).

2. THERMODYNAMICS

In the previous section, we have described the scaled NJL model. This section gathers results at finite temperature. We shall focus on analytical results for the thermodynamics. We shall then show our numerical results concerning the condensates and the thermodynamics in Section 3. We shall take parameters not necessarily in agreement with experiment but usefull to illustrate the meaning of some proposition. From this point of view, the NJL model is a very interesting toy model.

QCD has two phase transitions: a deconfinement transition corresponding to going from a hadronic gas to a quark-gluon plasma, and a transition leading to a phase where the chiral symmetry is restored. Lattice calculations [39, 40]

suggest that these two transitions coincide. In a purely gluonic theory, the (lattice) transition is of first order (for $N_c = 3$). However, when quarks are introduced, the order of the transition depends on the number of light flavors. With $N_f = 3$ massless flavors, QCD has a first order chiral transition, not connected to the pure gluonic one. When the mass of the quarks is varied, the two first order transitions are separated by a region in which there is a crossover. According to the type of calculations — Wilson fermions [41] or staggered (Kogut–Susskind) fermions [42] — QCD ($m_u \approx m_d \approx 10$ MeV, $m_s \approx 200$ MeV) appears to be in the first order region, or in the crossover region, respectively. It is then presently unclear which case occurs and we have the freedom to play with the parameters in such a way as to allow for both types of transitions*.

The deconfining transition is hard to study in existing models, although such models have been designed, *e.g.,* [48]. However, chiral symmetry breaking and its restoration can be studied in effective models. Both deconfinement and chiral symmetry restoration transitions are seen to be coincident on the lattice. In the following, we shall take the point of view that the study of the chiral phase transition can shed light on the deconfining transition. We shall also take the point of view that gluon confinement is linked to the gluon condensate χ_s, although this hypothesis is questionable [35, 49].

There is a constraint between the quark and gluon condensates, which shows up into the form of three coupled equations for the three condensates, see Eqs. (12)–(14). We can then get, according to the strength of this constraint, a first order transition (discontinuous passage from one phase to the other, see Fig. 2) or a second order transition (continuous transition from one phase to the other, see Fig. 3). (The pictures are shown in Section 3.) The analytical results given in this section have been discussed in [34, 50]. As already stated we work at the mean field level. The groups of Rostock [51, 52], Heildelberg [53–55] and Nikolov et al. [56] go beyond this approximation, studying the first $1/N_c$ corrections and showing that they are not negligible at low temperature and density (because pions are almost massless).

A. Pressure, Energy Density, Entropy Density, Bag Constant. In this section we want to understand the equilibrium properties of a strongly interacting matter, *i.e.,* determine the relations associated to the thermodynamics of a hot and dense system. The system is modelized by an effective action of the NJL type (free massive constituent quarks) with a dilaton field included**, Eq. (11). In a grand-canonical system, the partition function is given by

*Note that the distinction between pure gauge deconfinement and light quark chiral phase transition is of prime importance: the energy scales are different. Pure gauge transitions occur at a temperature of about 260 MeV while, with two light flavors, the critical temperature is around 150 MeV [39, 40, 43–45], or even as low as 140 MeV according to [46, 47].

**For the thermodynamics of a scaled linear sigma model, see [57] and references therein

$$\mathcal{Z} = \exp(-\beta \mathbf{\Omega}), \tag{15}$$

where $\mathbf{\Omega}$ is the thermodynamical potential (or grand potential). We exclusively consider a system in equilibrium: all the descriptions (micro-canonical, canonical, grand-canonical) are equivalent. However the grand-canonical description is the easiest. In the canonical formalism, the basic quantity is the Helmholtz free energy and the independent variables are the temperature, the pressure and the densities (one for each chemical potential). Since phase transitions occur at a constant chemical potential, and not at a constant density, it has always to be checked if a lower energy solution, obtained by separating the system into subsystems, exists [58]. Working in the grand-canonical formalism, where the independent variables are the temperature, the pressure and the chemical potentials, there is a direct access to the solutions corresponding to the minimum of the thermodynamical potential. Equation (15) leads to the identification

$$I_{\text{eff}} = \beta \mathbf{\Omega}. \tag{16}$$

Since [58, 59]

$$d\mathbf{\Omega} = -SdT - Pd\Omega - \rho_i d\mu_i \quad (i = u, d, s), \tag{17}$$

we get

$$P = -\left(\frac{\partial \mathbf{\Omega}}{\partial \Omega}\right)_{T,\mu_i}. \tag{18}$$

This implies

$$P = \frac{1}{\beta}\frac{\partial \ln(\mathcal{Z})}{\partial \Omega}\Bigg\}_{T,\mu_i}. \tag{19}$$

Physically, the pressure is not an absolute quantity. We have to consider it with respect to a reference system which is chosen to be the (nonperturbative) vacuum, of pressure P_0. Defining $P - P_0 = P'$ and replacing P' by P, we then have

$$P = \frac{1}{\beta}\frac{\partial \ln(\mathcal{Z}/\mathcal{Z}_0)}{\partial \Omega}\Bigg\}_{T,\mu_i}. \tag{20}$$

Subtracting the vacuum, the lowest order of the action is

$$I^s_{\text{eff}}(\varphi^s_a, \chi_s) \equiv I^s_{\text{eff}}(M_u, M_s, \chi_s) = I^s_{(\mu,\beta)}(M_u, M_s, \chi_s) + I^s_{(0,\infty)}(M_u, M_s, \chi_s) - I^s_{(0,\infty)}(M^0_u, M^0_s, \chi_0). \tag{21}$$

The first term is the Fermi part, which does not need being regularized,

$$I^s_{(\mu,\beta)}\left(M_u, M_s, \chi_s\right) = -\beta\Omega \frac{2N_c}{2\pi^2\beta} \sum_{i=u,s} a_i \int_0^\infty k^2 dk$$
$$\times \left\{ \ln\left(1+\exp\left[-\beta\left(E_i+\mu_i\right)\right]\right) + \ln\left(1+\exp\left[-\beta\left(E_i-\mu_i\right)\right]\right)\right\}, \quad (22)$$

where* $E_i = \sqrt{k^2+M_i^2}$, and $a_u = 2, a_s = 1$, while the Dirac part ($T = \mu = 0$) has to be regularized and is given by

$$I^s_{(0,\infty)}(M_u, M_s, \chi_s) - I^s_{(0,\infty)}(M_u^0, M_s^0, \chi_0) = -\beta\Omega \Bigg\{ \frac{2N_c}{32\pi^2} \sum_{i=u,s} a_i$$
$$\times \Bigg[(\Lambda\chi_s)^4 \ln \frac{(\Lambda\chi_s)^2 + {M_i}^2}{(\Lambda\chi_0)^2 + M_i^{0\,2}} - {M_i}^4 \ln \frac{(\Lambda\chi_s)^2 + {M_i}^2}{{M_i}^2}$$
$$+ M_i^{0\,4} \ln \frac{(\Lambda\chi_0)^2 + M_i^{0\,2}}{M_i^{0\,2}}$$
$$- \left(\frac{1}{2}(\Lambda\chi_s)^4 - \frac{1}{2}(\Lambda\chi_0)^4\right) + \left((M_i\Lambda\chi_s)^2 - (M_i^0\Lambda\chi_0)^2\right)\Bigg]$$
$$+ \Bigg[(\chi_s^4 - \chi_0^4)\Big(\frac{b^2}{16} + \frac{a^2}{4\chi_0^2}(\sigma_0^{s2} + \sigma_8^{s2})\Big)$$
$$- \sum_{i=u,s} a_i \Big(\frac{a^2\chi_s^2}{4} {M_i}^2 (1 - \frac{m_i}{M_i})^2 - \frac{a^2\chi_0^2}{4} M_i^{0\,2} (1 - \frac{m_i}{M_i^0})^2\Big)$$
$$- \frac{b^2}{16}\chi_s^4 \ln\left(\frac{\chi_s}{\chi_0}\right)^4 \Bigg]\Bigg\}. \quad (23)$$

With the action (21), Eq. (20) gives

$$P = -\frac{1}{\beta} \frac{\partial I^s_{\rm eff}(M_u, M_s, \chi_s)}{\partial\Omega}, \quad (24)$$

which leads to

$$P = -\frac{1}{\beta\Omega}\Big[I^s_{(\mu,\beta)}(M_u, M_s, \chi_s) +$$
$$+ I^s_{(0,\infty)}(M_u, M_s, \chi_s) - I^s_{(0,\infty)}(M_u^0, M_s^0, \chi_0)\Big]. \quad (25)$$

*When no confusion is possible between the 4-momentum k and the 3-momentum $\vec{k}$, we use the notation k for $|\vec{k}|$.

The physical meaning of this equation is that the grand potential is an extensive quantity:

$$\mathbf{\Omega} = -P\Omega. \tag{26}$$

Mathematically, the mean field approximation corresponds to finding the minimum of the action. Equation (26) shows the physics attached to this condition: the system chooses the phase where the pressure is a maximum.

Quark densities can be evaluated from (17) and are given by

$$\rho_i = -\left(\frac{\partial \mathbf{\Omega}}{\partial \mu_i}\right)_{T,\Omega} = -\frac{1}{\beta\Omega}\left(\frac{\partial I^s_{\text{eff}}}{\partial \mu_i}\right) = -\frac{N_c}{\pi^2}\int_0^\infty k^2\left(n_{i+} - n_{i-}\right)dk, \tag{27}$$

where

$$n_{i\pm} = \frac{1}{1+\exp\left[\beta\left(E_i \pm \mu_i\right)\right]}. \tag{28}$$

If we work in the isospin limit ($m_u = m_d$) for a symmetric matter ($\mu_u = \mu_d$), it is clear that $\rho_u = \rho_d$.

The entropy density can also be evaluated from (17) and is given by

$$s \equiv \frac{S}{\Omega} = -\frac{1}{\Omega}\left(1 - \beta\frac{\partial}{\partial\beta}\right) I^s_{(\mu,\beta)}\left(M_u, M_s, \chi_s\right). \tag{29}$$

Only the Fermi part appears in this formula since this is the only one which depends upon temperature. When $T \to 0$ the entropy density s goes to zero, in agreement with the third principle of thermodynamics.

Finally, the internal energy is given by [58, 59]

$$\begin{aligned} E \equiv \mathbf{\Omega} + TS + \mu_i\rho_i &= \left(1 + \beta\frac{\partial}{\partial\beta} - \mu_i\frac{\partial}{\partial\mu_i}\right)\mathbf{\Omega} = \\ &= \left(\frac{\partial}{\partial\beta} - \frac{1}{\beta}\mu_i\frac{\partial}{\partial\mu_i}\right) I^s_{\text{eff}}(M_u, M_s, \chi_s). \end{aligned} \tag{30}$$

This gives the energy density

$$\begin{aligned} \epsilon \equiv \frac{E}{\Omega} \;=\; & \frac{1}{\Omega}\left(\frac{\partial}{\partial\beta} - \frac{1}{\beta}\mu_i\frac{\partial}{\partial\mu_i}\right) I^s_{(\mu,\beta)}\left(M_u, M_s, \chi_s\right) \\ + \; & \frac{1}{\beta\Omega}\left[I^s_{(0,\infty)}\left(M_u, M_s, \chi_s\right) - I^s_{(0,\infty)}\left(M^0_u, M^0_s, \chi_0\right)\right]. \end{aligned} \tag{31}$$

Like the pressure, the energy density is a relative quantity: (31) gives the density energy of the system w.r.t. the vacuum energy.

B. Bag Constant B. Following [47,60], we write

$$P = P_{\text{ideal gas}} - B(\beta, \mu_u, \mu_s), \tag{32}$$

$$\epsilon = \varepsilon_{\text{ideal gas}} + B(\beta, \mu_u, \mu_s), \tag{33}$$

$$Ts = P_{\text{ideal gas}} + \varepsilon_{\text{ideal gas}} - \mu_i \rho_i, \tag{34}$$

with

$$P_{\text{ideal gas}} = -\frac{I^s_{(\mu,\beta)}(M_u, M_s, \chi_s)}{\beta\Omega} =$$

$$= \frac{N_c}{3\pi^2} \sum_{i=u,s} a_i \int_0^\infty \frac{k^4}{E_i} (n_{i+} + n_{i-})\, dk, \tag{35}$$

$$\varepsilon_{\text{ideal gas}} = \frac{1}{\Omega}\left(\frac{\partial}{\partial\beta} - \frac{1}{\beta}\mu_i \frac{\partial}{\partial\mu_i}\right) I^s_{(\mu,\beta)}(M_u, M_s, \chi_s)$$

$$= \frac{N_c}{\pi^2} \sum_{i=u,s} a_i \int_0^\infty k^2 E_i (n_{i+} + n_{i-})\, dk, \tag{36}$$

being quantities relative to a massive free quark system. The interaction measure, which is an indication of nonperturbative effects, is

$$\varepsilon - 3P = 4B + \frac{N_c}{\pi^2} \sum_{i=u,s} a_i M_i^2 \int_0^\infty \frac{k_i^2}{E_i} (n_{i+} + n_{i-})\, dk. \tag{37}$$

In Eqs. (32) and (33), we have defined a temperature and density dependent (through M_u, M_s, χ_s) bag constant* B. It depends on the Dirac contribution (23) to the pressure:

$$B(\beta, \mu_u, \mu_s) = \frac{1}{\beta\Omega}\left\{ I^s_{(0,\infty)}(M_u, M_s, \chi_s) - I^s_{(0,\infty)}\left(M_u^0, M_s^0, \chi_0\right)\right\}. \tag{38}$$

The definition (38) is different from [30,37,54,61] because two new effects are implemented: *i*) we take into account the explicit breaking of chiral symmetry (even if $m_u = 0$, we have $m_s \neq 0$: the strange quark contribution can be nonnegligible); *ii)* as already stated, Eq. (38) takes into account the effects of the gluons. Moreover, (38) conceptually differs from the definition [54] where the bag constant is zero in the chirally restored phase. Finally, it is different from the bag constant B' introduced in [29,31,38]. In these references, it is only obtained

*In [47,60], there is no glueball: the bag constant is purely chiral. Our bag constant is then a generalization of these references.

at zero temperature and density, through the definition of B', being identical to the energy difference between the perturbative vacuum and the true vacuum*.

In the perturbative vacuum, the chiral symmetry is restored and the gluon condensate vanishes. Then, according to [29],

$$B' = \frac{1}{\beta\Omega}\left\{I^s_{(0,\infty)}\left(0,0,0\right) - I^c_{(0,\infty)}\left(M^0_u, M^0_s, \chi_0\right)\right\} = \frac{1}{16}m^2_{GL}\chi^2_0, \tag{39}$$

with $m^2_{GL} = b^2\chi^2_0$. In $SU(3)$, implementing $m_s = 0$ in the definition of the perturbative vacuum makes no sense. However, we shall see that the value of $B'^{1/4}$ is not so far from that of $B^{1/4}$ (38) (for $T >>$) so that the use of (39) in [29, 31, 38] is verified *a posteriori*. This remark also applies for the effect of χ_s which does not go down to zero.

Note that in [61], the authors study both the chiral symmetry restoration and the effects of the gluon condensate. They however define two bag constants, one associated to the restoration of scale symmetry, the other to the restoration of chiral symmetry.

C. High Temperature Zero Density Limit ($T > T_c$). In a phase where chiral symmetry is restored — in this section, we mean the phase where the constituent quark mass goes to the current quark mass ($M_i = m_i$, $i = u, s$) even if we are not in the chiral limit — we have $m_s/T \lesssim 1$: a high temperature expansion in m_s/T is possible [50, 62, 63]. Calculations are lengthy and left to Appendix A. We work at zero density. Our results are a generalization of the latter references where only a limited number of terms in the m_s/T expansion have been retained while we are able to give here the full expansion, involving only elementary functions. Note that to describe the results in Section 3, the first four terms will be enough ($T > T_c$, with T_c the critical temperature) so that we only keep them in the following. For the pressure, we get

$$P_{\text{ideal gas}} \approx T^4\left(\frac{7}{60}N_c\pi^2 - \frac{N_c}{12}\frac{m^2_s}{T^2} - \frac{N_c}{8\pi^2}\frac{m^4_s}{T^4}\ln\frac{m_s}{\pi T} + \right.$$

$$\left. + \frac{N_c}{16\pi^2}\left(\frac{3}{2} - 2\gamma\right)\frac{m^4_s}{T^4} + \ ...\right), \tag{40}$$

where γ is the Euler constant**.

*One can also take the equivalent definition of considering it only through the glueball Lagrangian (decoupling between the glueball and the other fields). We have $B = \frac{1}{4} < \theta_{\mu\mu} >= = \frac{b^2}{16}\chi^4 = \frac{1}{16}m^2_{GL}\chi^2$.

**In [54], the massless free quark limit is unreachable, by construction: the d^3k regularization introduces a cut-off Λ for each Fermi or ideal gas quantity. These quantities, for example $P_{\text{ideal gas}}$, behave then at high temperature as Λ/T, decreasing to zero. This drawback is not present in this work, where we have chosen a d^4k regularization for the vacuum while the Fermi part is not regularized.

Note that the case of finite chemical potentials is much more complex and, to our knowledge, has never been treated to all orders in the fermionic case. (In the bosonic case, the constraint $\mu_i < M_i$ (not present in the fermionic case) allows a high temperature expansion (m_i/T and $\mu_i/T \lesssim 1$) to all orders [64–66].)

Above T_c, the bag constant B is temperature independent and writes

$$B = \frac{1}{\beta\Omega}\left\{I^s_{(0,\infty)}\left(0, m_s, \chi_c\right) - I^s_{(0,\infty)}\left(M^0_u, M^0_s, \chi_0\right)\right\}, \tag{41}$$

where χ_c is the gluon condensate above T_c. Note that, for any set of parameters (M^0_u, χ_0), we could not get $\chi_c = 0$. In our model there is never a complete gluon deconfinement. This is related to the fact that gluons are only poorly incorporated in our formalism (we have no explicit temperature dependence of the gluon condensate since the modeling of the gluon anomaly is through a temperature independent potential (see last term of Eq. (11)); we also do not have the right number of gluonic d.o.f.).

The energy density is given by (31), so that

$$\varepsilon_{\text{ideal gas}} = \frac{1}{\Omega}\frac{\partial I^s_{(\mu,\beta)}}{\partial\beta}, \tag{42}$$

i.e., using (16) and (26),

$$\varepsilon_{\text{ideal gas}} = -\frac{\partial}{\partial\beta}(\beta P_{\text{ideal gas}}). \tag{43}$$

With (40), the high temperature, zero density, expansion gives (Appendix A)

$$\varepsilon_{\text{ideal gas}} \approx T^4\left(\frac{7}{20}N_c\pi^2 - \frac{N_c}{12}\frac{m_s^2}{T^2} + \right.$$

$$\left. + \frac{N_c}{8\pi^2}\frac{m_s^4}{T^4}\ln\frac{m_s}{\pi T} + \frac{N_c}{16\pi^2}\left(2\gamma + \frac{1}{2}\right)\frac{m_s^4}{T^4} + \ ...\right). \tag{44}$$

Finally, (16) and (26) applied to (29) lead to

$$s = \left(1 - \beta\frac{\partial}{\partial\beta}\right)\beta P_{\text{ideal gas}}, \tag{45}$$

or, equivalently, to

$$s = -\beta^2\frac{\partial}{\partial\beta}P_{\text{ideal gas}} = \frac{\partial}{\partial T}P_{\text{ideal gas}}. \tag{46}$$

The high temperature, zero density, expansion of the entropy density is then (Appendix A)

$$Ts \approx T^4\left(\frac{7}{15}N_c\pi^2 - \frac{N_c}{6}\frac{m_s^2}{T^2} + \frac{N_c}{8\pi^2}\frac{m_s^4}{T^4} + ...\right). \tag{47}$$

The results (40), (44) and (47) are used in Section 3.

D. Low Temperature Zero Density Limit. To simplify the discussion, we limit ourselves to the zero density case. If M_u^0 is of the order of 400 MeV, the low temperature expansion (see Appendix A) is valid up to $T \approx 100$ MeV. Indeed, masses and condensates are not varying within this range of temperatures, see Section 3, and the expansion parameters βM_u and βM_s are then large enough — we have at worst $\beta M_u \approx 4$ — to allow a stationary phase expansion of (35):

$$P_{\text{ideal gas}} \approx \frac{4N_c\beta^{-5/2}}{(2\pi)^{3/2}} \sum_{i=u,s} a_i M_i^{3/2} e^{-\beta M_i} \; + \; \text{corrections}, \tag{48}$$

where $a_u = 2, a_s = 1$. To get the corrections*, it is better to work with (35) written in terms of K_2, of which the asymptotic behavior is well known. The method is explained in Appendix A which also contains the low temperature zero density expansion of the energy and entropy densities.

The results relative to this section are given in Section 3B. They necessitate the knowledge of the behavior of the condensates as a function of temperature, given in Section 3A.

3. RESULTS

We show the variation as a function of temperature of the quark and gluon condensates in Section 3A. We then discuss the results relative to the thermodynamics in Section 3B.

A. Condensates. The quark and gluon condensates are given by

$$\begin{aligned} \langle \bar{u}u \rangle \; &\equiv \; \frac{1}{\beta\Omega} \frac{\partial I^c_{\text{eff}}}{\partial m_u} (M_u, M_s, \chi_s) = \\ &= \; -\frac{1}{2} a^2 \chi_s^2 (M_u - m_u) = -4N_c M_u g_{M_u,\beta,\mu_u}, \end{aligned} \tag{49}$$

$$\begin{aligned} \langle \bar{s}s \rangle \; &\equiv \; \frac{1}{\beta\Omega} \frac{\partial I^c_{\text{eff}}}{\partial m_s} (M_u, M_s, \chi_s) = \\ &= \; -\frac{1}{2} a^2 \chi_s^2 (M_s - m_s) = -4N_c M_s g_{M_s,\beta,\mu_s}, \end{aligned} \tag{50}$$

and by Eq. (14). The constituent quark masses M_u and M_s used in these equations come from the gap equations (12), (13). When $m_u = 0$, $M_u = 0$ is always a solution of (12), so that it has to be checked if it corresponds to a greater pressure.

*Corrections to (48) are negligible only if $\beta M_i \gtrsim 40$. However their number is limited for βM_i as low as 4. In Appendix A, we quantitatively discuss the importance of these corrections with respect to the value of βM_i.

We define a second order transition to be a transition for which the slope of the pressure as a function of the external parameters T, μ is continuous (this includes both true second order transitions and crossovers); otherwise it is said to be of the first order. Different behaviors show up according to the chosen set of (model) parameters and to the external (temperature and density) parameters: we can have two first order transitions, coincident or not, or two second order transitions. We can also have a second order transition for one species of quark while the other experiences a first order transition.

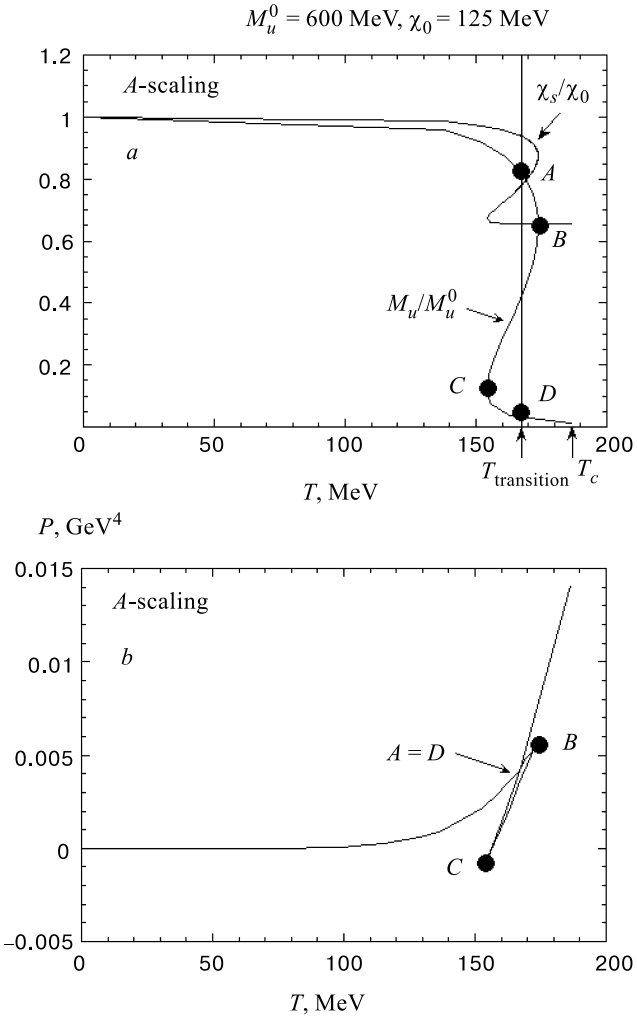

Fig. 2. Up constituent quark mass transition (with $m_u \neq 0$)

A discontinuous slope for the pressure means a discontinuous condensate: there is a mass gap. This is illustrated in Fig. 2.

Since the pressure at point A is identical to the pressure at point D, the transition takes place between these two points. Only the region from B to C is unstable: there is metastability between A and B and between C and D.

Note that looking graphically at the pressure to find the transition point is manageable only in the two degenerate flavor model at zero density or temperature. In that case, the strategy is the following. Given M_u, the corresponding χ_s can be extracted from Eq. (14) with the strange quark contribution removed (two-flavor case). We can then use this couple (M_u, χ_s) to extract the corresponding temperature from the gap equation, Eq. (12). There is only one solution. (Should we have fixed the temperature, we should have to solve two coupled equations (12),(14) with the problem that, for a first order transition, several solutions are possible.) We then get the ABCD curve of Fig. 2(a). To get the transition point it is then enough to look at the pressure, Fig. 2(b).

Of course, as soon as more variables (μ_u, μ_s, M_s) are introduced, this strategy is not anymore of interest. We have to solve the full set of coupled equations (12)–(14) as a function of chemical potentials and temperature. Because of possible first order transitions, several local extrema of the pressure show up so that it is necessary to use a numerical algorithm searching for global extrema. In our work [50], we used the simulated annealing algorithm that we adapted from [67].

In order to save place, we restrict ourselves to two sets of parameters:

$$(i) \quad M_u^0 = 300 \text{ MeV}, \ \chi_0 = 80 \text{ MeV}, \tag{51}$$

$$(ii) \quad M_u^0 = 600 \text{ MeV}, \ \chi_0 = 125 \text{ MeV}. \tag{52}$$

Figure 3 is for the set (51) and corresponds to a second order phase transition w.r.t. the temperature for vanishing chemical potentials. It is similar to results obtained in the two-flavor case [29, 31]. The choice $M_u = 350$ MeV, $\chi_0 = 450$ MeV would almost corresponds to a pure NJL model with a critical temperature of $T_c \approx 193$ MeV. The gluon condensate is almost flat, so that the quark and gluon condensates are almost uncoupled. In contrast, the choice (51) leads to a greater coupling between condensates and the critical temperature is lowered ($T_c \approx 150$ MeV in the chiral limit*, see Fig. 4). Such a low temperature is in agreement with lattice results [40, 45–47].

Working in the three-flavor version of the model, these two pictures show also the strange quark condensate, for which we can make two remarks:

• $< \bar{s}s >$ decreases slower than $< \bar{u}u >$, in agreement with [68]. This can be traced back to the greater constituent strange quark mass compared to the up

*The two-flavor case leads to a critical temperature of 140 MeV.

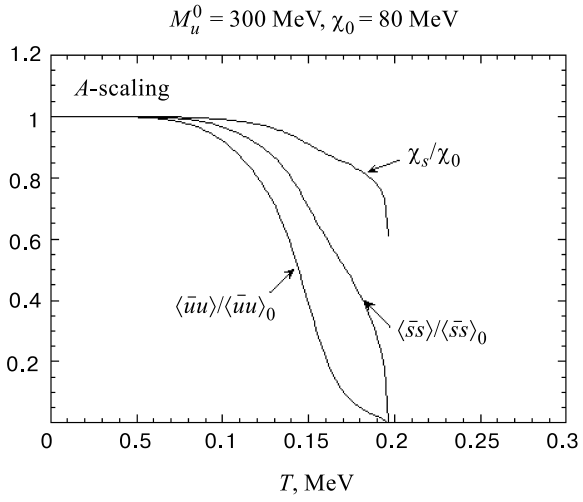

Fig. 3. Quark and gluon condensates as a function of temperature for the parameters $M_u^0 = 300$ MeV, $\chi_0 = 80$ MeV*

quark which, in turn, is a consequence of a greater current strange quark mass compared to the up one**. Note however that our results show a faster decrease of $< \bar{s}s >$ with temperature than in [69];

• Because of the coupling between the condensates, the gluon condensate at the transition, χ_c, is smaller than in the two-flavor case. For the set (51), we have $\chi_c(SU(2)) \approx 0.8$ while Fig. 3 shows $\chi_c(SU(3)) \approx 0.6$.

Figure 5 is the analogue of Fig. 3 for the set of parameters (52). This set allows one to get a first order phase transition [29, 38]. The coupling between quark and gluon condensates is so strong that all the condensates undergo the transition together. At zero density, the above analysis shows that:

• We can reproduce both first and second order phase transitions. A first order transition is typically an effect due to the gluon condensate which then does not show up in pure NJL models;

• A low critical temperature, as low as 140 MeV, can be reproduced. This is clearly related to the coupling between quark and gluon condensates. Pure

*Pictures 3,5–8 are reprinted from
• Nuclear Physics A582, M.Jaminon, B. Van den Bossche, «$SU(3)$ Scaled Effective Lagrangians for a Hot and Strange System», p.517–567, Copyright 1995.
• Nuclear Physics A582, M.Jaminon, B. Van den Bossche, «Phase Transition and Thermodynamics of a Hot and Dense System in a Scaled NJL Model», p,515–538, Copyright 1996
with permission from Elsevier Science.

**Note that, in the two-flavor limit, where $M_s, m_s \to \infty$, we have $< \bar{s}s > / < \bar{s}s >_0 = 1$.

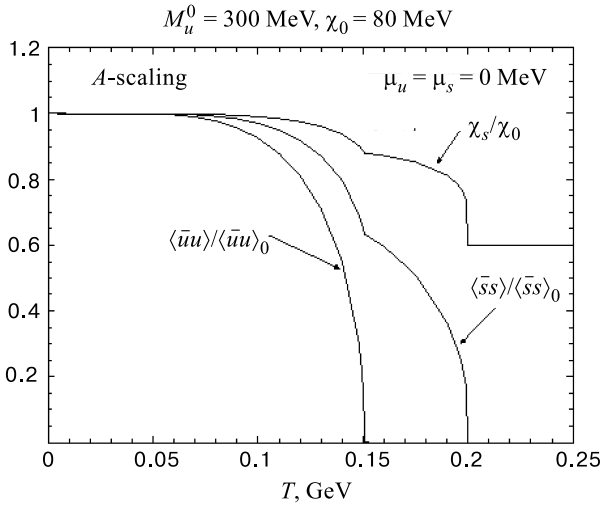

Fig. 4. Quark and gluon condensates as a function of temperature for the parameters $M_u^0 = 300$ MeV, $\chi_0 = 80$ MeV in the light quark chiral limit $m_u = m_d = 0$ MeV

NJL models are then unable to reproduce such a low temperature: they cannot go below $T_c \approx 190$ MeV. In fact, it can be shown from the gap Equation (12) that the critical temperature is given by (for a second order phase transition in the two-flavor case)

$$T_c = \sqrt{\frac{3}{2}}\frac{\Lambda\chi_c}{\pi}\left(1 - \frac{8\pi^2 a^2}{4N_c\Lambda^2}\right)^{1/2}. \tag{53}$$

According to this equation, scaled models allow (for second order transitions) a reduction of the critical temperature in the ratio χ_c/χ_0 compared to a pure NJL model;

• The coupling between quark and gluon condensates is mainly driven by the value of the vacuum gluon condensate χ_0. With large χ_0, the coupling is weak while the coupling becomes more and more important as we decrease χ_0. The quark or gluon condensate can then be considered as the order parameter for the phase transition.

It should however not be forgotten that all the above analysis is performed without vector mesons. Without them, our results show that high values of the gluon condensate are needed to get a transition above the normal nuclear matter density ρ_0, see Fig. 5 of [31].

Although the scaled models are not able to reproduce a transition above the normal nuclear density for a small value of the gluon condensate (which leads to a low critical temperature), it does not mean that they are inefficient. Indeed, it

is well known that vector mesons make the vacuum stiffer against the restoration of chiral symmetry [71,72]. Including these mesons will then correct what seems to be, at first sight, a drawback of the model.

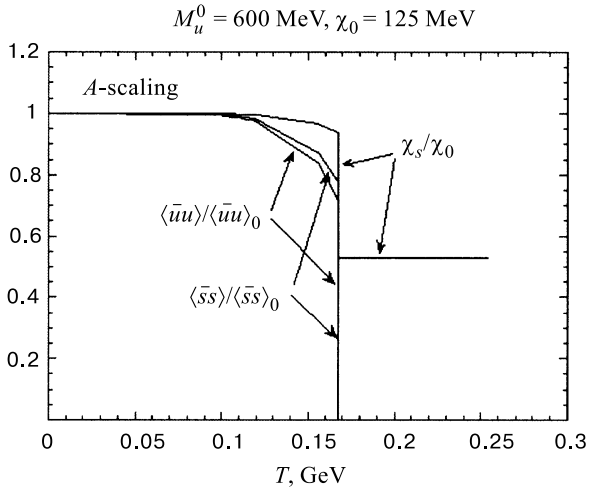

Fig. 5. Quark and gluon condensates as a function of temperature for the parameters $M_u^0 = 600$ MeV, $\chi_0 = 125$ MeV

B. Thermodynamics. In this section, we present results relative to the pressure (equation of state), the energy density and the entropy density that we have adapted from [34, 50]. Because we would like to emphasize some points relative to fits, we first take the somehow unusual way to present these quantities as a function of T^4 (pressure, energy density) or T^3 (entropy density). This allows us to separate curves corresponding to different parameters. Once these results will have been presented, we shall redraw some of our results in the usual way (pressure or energy density or T times the entropy density, over T^4, as a function of T), allowing us to make a more direct comparison with the general shape of these quantities as obtained in lattice calculations. Pressure, energy and entropy densities are obtained from (25), (31), and (29), respectively. The general behavior of these quantities can be understood (at vanishing density) from Eqs. (32)–(34) with asymptotic behaviors given in Appendix A and summarized in Sections 2C and 2D.

Pressure. The behavior of the pressure is shown in Fig. 6*(a)* for a vanishing density. As the strange quark mass m_s is different from zero, the behavior of the pressure above T_c is not the usual T^4 law: in addition to the bag constant (41) which is taken into account through the decomposition (32), the massive free gas part has the temperature expansion (40).

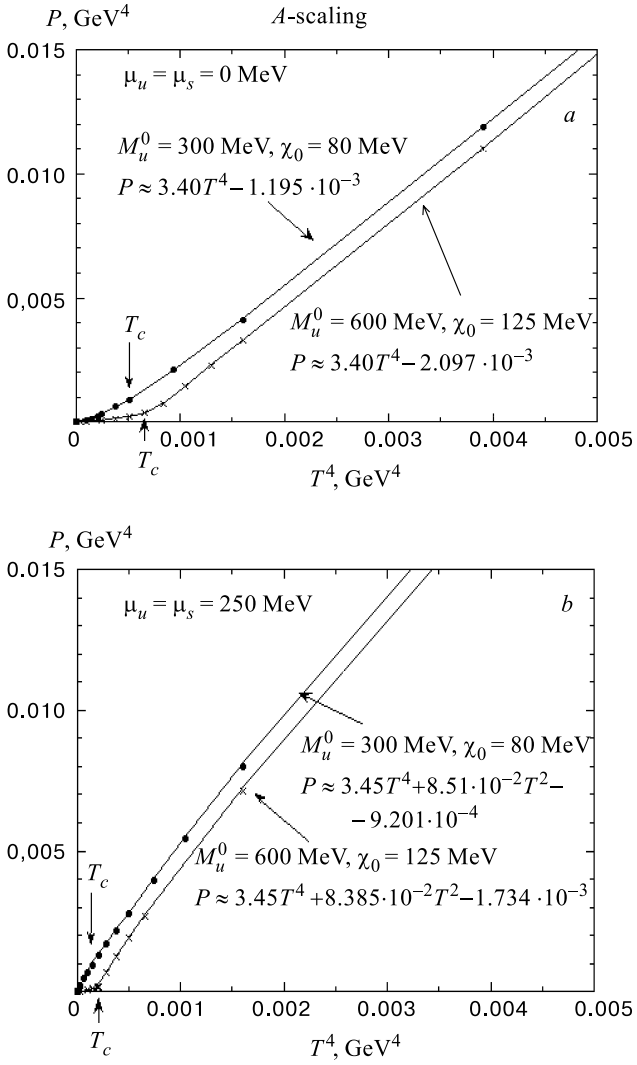

Fig. 6. Pressure as a function of T^4 for the set of parameters (51,52) for $\mu_u = \mu_d = \mu_s = 0$ MeV *(a)*; for $\mu_u = \mu_d = \mu_s = 250$ MeV *(b)*

Figure 6*(a)* shows also the linear fit in T^4 which is valid in the phase where the chiral symmetry is restored:

$$P \approx 3.40\ T^4 - 1.195\ 10^{-3} \tag{54}$$

for the set (51), and

$$P \approx 3.40\ T^4 - 2.097\ 10^{-3} \tag{55}$$

for the set (52). Note that the coefficient of T^4 is not equal to the coefficient $7N_c\pi^2/60$ (=3.454) of the term T^4 in the expansion (40). Because of the limited range of temperatures investigated in Fig. 6, the corrective terms to the factor T^4 in the expansion (40) change the apparent slope, and the constant term in (54) cannot be identified with the bag constant B. When a fit is realized with all the terms* of the expansion (40), plus a constant C to adjust, this one equals $C^{1/4} \approx 179$ MeV for the set (51) and $C^{1/4} \approx 207$ MeV for the set (52). These values are close to $B^{1/4} \approx 183$ MeV (set (51)) and $B^{1/4} \approx 209$ MeV (set (52)) obtained from a direct calculation of the exact bag constant (41). This shows the consistency of our numerical results and the fast convergence of the expansion (40), even if the expanding parameter m_s/T is not so small! Note also that the numerical values of $B^{1/4}$ extracted from the exact bag constant (41) or extracted from the fits are not so far from $B'^{1/4}$ given by the approximate Equation (39). The latter is valid if we ignore the coupling between the quark and gluon condensates, and gives $B'^{1/4}$ = 161 MeV (set (51)) and $B'^{1/4}$ = 201 MeV (set (52)). This justifies *a posteriori* the introduction of the approximate bag constant (39) in the references [29, 30, 38]**.

This discussion shows that it could be quite dangerous to extract numerical values from fits: one could be tempted to identify the bag constant from the constant term in (54) and (55). The above analysis shows clearly that it would be wrong.

Beyond the transition, the behavior of the pressure versus temperature depends on the order of the transition. For the set (52), βM_i ($i = u$, s) remains quite large, so that the T behavior is described in a first approximation by (48). However, a careful analysis shows that this expansion is not well suited for $\beta M_s \leq 20$, or even for $\beta M_s \leq 40$, and that the expansion (A35) should be used instead. The exponential behavior $e^{-\beta M_s}$ is however still correct. For the set (51), the phase transition is of second order so that M_u is progressively decreasing. This implies that the expansion (A35) cannot be used over the whole range $T < T_c$ and, even more, that it is too crude to describe this behavior. We have however found that the expansion (A34), with the sum limited to $n = 1$ and $n = 2$, is well suited for temperatures below 100 MeV.

*By all the terms we mean the terms which are included in (40). Indeed the precision is sufficient and we do not have to take into account more terms defined in (A32).

**It should however be stressed that it is better to work with the exact expression since an error in $B^{1/4}$ is amplified when going to B.

Note that for an analysis based on the $1/N_c$ expansion [51,53–55,74], it has been shown that the pions give the largest contribution to the thermodynamical quantities at low temperature*. In the chiral limit where the pions are massless, their behavior is in T^4, which effectively shows they have a bigger contribution than (48) based on the high constituent quark mass. This is an example where the $1/N_c$ approach to the lowest order is not valid (see [6]).

The above analysis shows that an important ingredient is not included: indeed, the T^4 obtained for $P_{\text{ideal gas}}$ does not contain the gluonic d.o.f., as indicated previously. In the chiral limit, we should have

$$P_{\text{ideal gas}} = \frac{\pi^2}{90}\left\{2N_g + \frac{7}{8}N_c N_f 4\right\}T^4 \approx 5.2\ T^4, \tag{56}$$

with N_g = 8 if N_c = 3.

Although the gluon condensate is in part due to these gluonic d.o.f., gluons do not contribute to the thermodynamics. To take into account the thermodynamics of a purely gluonic system, we should add to the Lagrangian (11) a temperature dependent potential $V_\chi(T)$. This has for example been noticed in [37, 77, 78]. The choice of this potential should be such that it leads to the behavior (56).

Figure 6*(b)* is the analogue of figure 6*(a)* for the choice $\mu_u = \mu_s$ = 250 MeV. These values correspond to a strong coupling between the condensates $<\bar{u}u>$ and $<\bar{s}s>$ for the set (52), and to a weak coupling for the set (51). With a chemical potential, there is no possible T^4 linear fit. This can be seen considering the chiral limit ($m_u = m_d = m_s = 0$) of (32) with (35). This leads to

$$P = \frac{7}{60}N_c\pi^2T^4 + \frac{N_c}{2}\mu^2T^2 + \frac{N_c\mu^4}{4\pi^2} - B. \tag{57}$$

Because $m_s \neq 0$, Eq.(57) has to be modified. Figure 6(b) shows that the T^4 part is not modified compared to (57), while the T^2 part is slightly smaller. Once again, this shows that one has to be very careful when making fits. The coefficient of the T^4 term is not identical to the one of (54): the supplementary terms in (40), and terms coming from the chemical potential, have a repercussion upon all the terms of the fit.

Energy. The behavior of the energy density versus temperature, as given by (33) and (36), is represented in Fig. 7. At high temperature and for vanishing density, the whole expansion (A37) can be restricted to the first four terms (44), which perfectly describe the curves above the chiral transition. For the sets (51) and (52), we get the linear T^4 fits

$$\varepsilon \approx 10.271\ T^4 + 0.877\ 10^{-3} \tag{58}$$

*This is in agreement with the results [75] based on chiral perturbation theory [76].

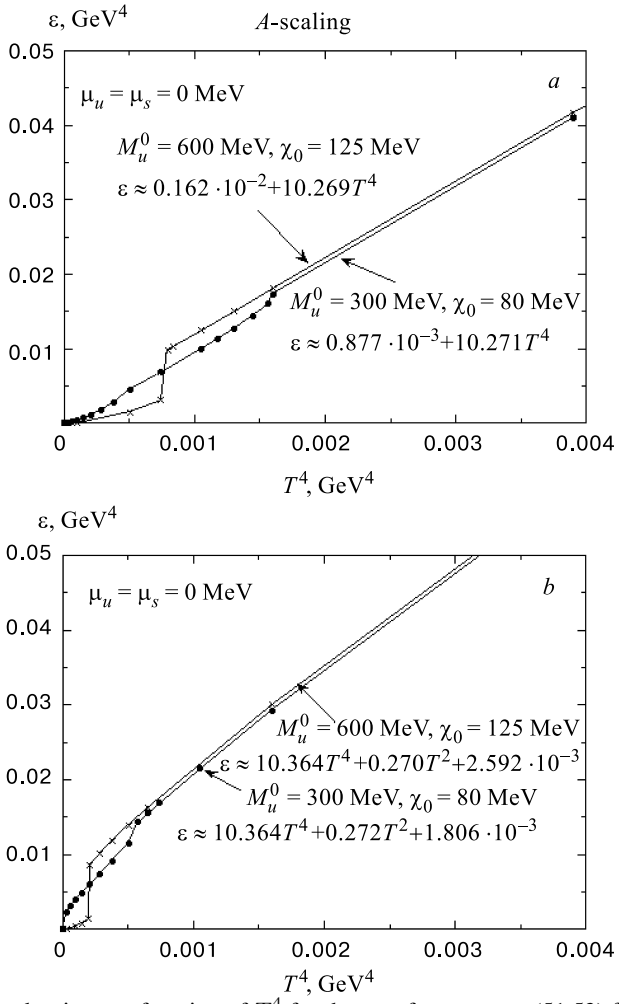

Fig. 7. Energy density as a function of T^4 for the set of parameters (51,52) for $\mu_u = \mu_d = \mu_s = 0$ MeV *(a)*; for $\mu_u = \mu_d = \mu_s = 250$ MeV *(b)*

and

$$\varepsilon \approx 10.269\ T^4 + 1.620\ 10^{-3}, \tag{59}$$

respectively.

It is useful to stress once more the difficulties one encounters to extract meaningful information form fits such as (58) and (59), since the constant terms in (58) and (59) are not the opposite of (54) and (55), while the exact Eqs. (32) and (33) show clearly that they should. In fact, all the terms from the expansion

(44) contribute to the determination of the coefficients of the fits in the restricted range of temperatures investigated.

The expansion (44) is perfectly adequate since a fit from its different terms plus a constant C to be adjusted gives $C^{1/4} \approx 182$ MeV for the set (51) and $C^{1/4} \approx 208$ MeV for the set (52), in excellent agreement with the results obtained from the behavior of the pressure. Figure 7 shows that the order of the transition and the nature of the coupling (strong or weak) between the quark condensates are very well visualized with the help of the energy density curves: there is a jump at T_c if the transition is of first order, while there is a change of slope quite visible if it is a true* second order transition.

This is the case for the set (51), see Fig. 4: the transition is of second order for the up quarks while the strange quarks feel a first order transition. There is then a change of the slope of $\varepsilon(T)$ at T_{uc} and an energy jump at T_{sc}, see Fig. 7*(a)*.

The behavior below the transition can be understood from Eq. (A39), with the same restrictions as in the case of the pressure, for the corresponding set of parameters.

Figure 7*(b)* is the analogue of Figure 7*(a)* for $\mu_u = \mu_s$ = 250 MeV. Chemical potentials introduce a T^2 dependence in the simpler case of chiral limit. We have, with $\mu \equiv \mu_u = \mu_s$,

$$\varepsilon = \frac{7}{20} N_c \pi^2 T^4 + \frac{3}{2} N_c \mu^2 T^2 + \frac{3}{4} N_c \frac{\mu^4}{\pi^2} + B. \tag{60}$$

This equation comes from (36) or, more directly, from (31) together with (16) and (26). Figure 7*(b)* shows also that having m_s different from zero does not affect too much the second term of (60), and introduces a constant supplementary term. All the remarks concerning the fits are also valid here.

Entropy. For a massless free quark gas, the entropy density behaves like T^3. Since the strange current quark mass does not vanish, the high temperature expansion has correcting terms. Equations (34), (40) and (44) give the first three terms of Ts (temperature times the entropy density) in powers of T^2, leading to Eq. (47). The complete expansion is given by (A43).

Figure 8*(a)* shows that Eq. (47) can be approached by a linear expression in T^3 in the given range of temperatures:

$$s \approx 13.839\ T^3 - 0.912\ 10^{-2}, \tag{61}$$

and

$$s \approx 13.868\ T^3 - 0.136\ 10^{-1}, \tag{62}$$

for the set of parameters (51) and (52), respectively.

*We mean a transition which is not a crossover, *i.e.*, we are in the chiral limit.

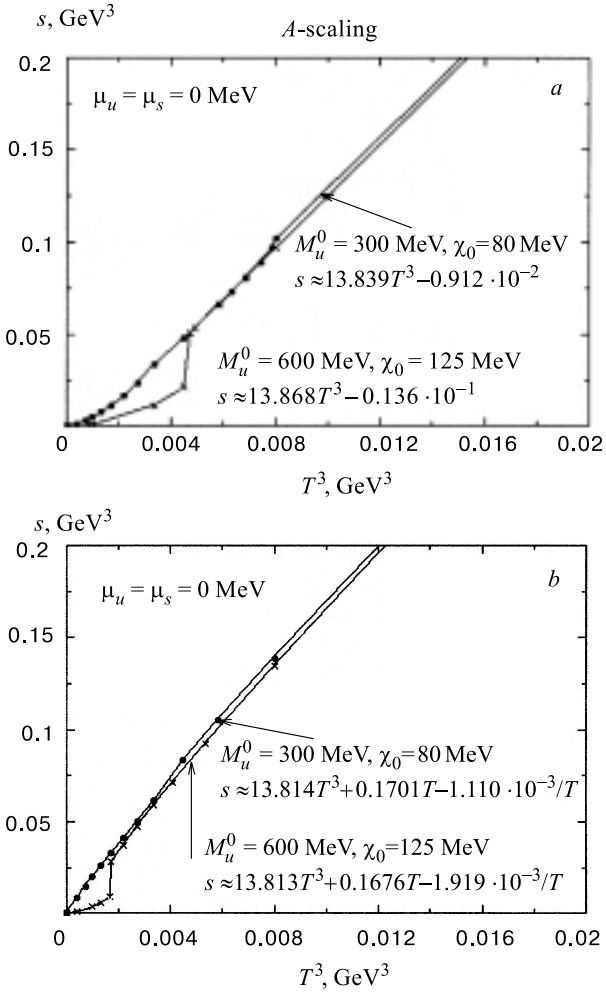

Fig. 8. Entropy density as a function of T^3 for a set of parameters (51,52) for $\mu_u = \mu_d = \mu_s = 0$ MeV *(a)*; for $\mu_u = \mu_d = \mu_s = 250$ MeV *(b)*

Although the numerical results seem to fit exactly the relation (29), the T^3 coefficients of (61) and (62) do not correspond to the combination of Eqs. (54), (55), (58), (59). This remark confirms once more what we claimed in the pressure and energy density case: it is dangerous to extract information from fits if we do not take care of possible corrections. In our case, fits in T^4 (for pressure and energy) and in T^3 (for entropy) do not help to get the bag constant or the number of excited d.o.f. The more complete forms (40), (44), and (47) have to be considered.

The behavior of the entropy below the chiral transition can be understood using (A45) with the same warning as in the pressure case, for the corresponding set of parameters.

Figure 8*(b)* shows the entropy behavior for nonvanishing chemical potentials. Using Eqs. (34), (57), and (60), and the density (27) in the limit where all masses are vanishing

$$\rho \equiv \sum_i \rho_i = \frac{N_c \mu^3}{\pi^2} + N_c \mu T^2, \tag{63}$$

we get

$$Ts = \frac{7}{15} N_c \pi^2 T^4 + N_c \mu^2 T^2, \tag{64}$$

which has to be modified in order to take into account the finite value of m_s. It is worth noticing that m_s only slightly affects the T^2 term of (64).

As a conclusion to these results, we can mention that, above the chiral transition, all the d.o.f. of the model are excited. However the vanishing mass limit of QCD is not reached for two reasons [70]:

• The gluon d.o.f. are not included at high temperature. A temperature and density dependent potential $V_\chi(T, \mu)$ should be taken into account;

• The strange quark mass is not negligible. We need going to very high temperatures in order that the lowest term in T^4 subsists in the expansion m_s/T.

We should also notice that the $1/N_c$ corrections in references [51, 53–55, 74] show that the low temperature thermodynamics is driven by pion motion, pions being much lighter than the constituent quark mass. Since the quark loop contribution takes into account thermal excitations of quarks with mass $M \gtrsim 300$ MeV (whose probability is reduced by the Boltzmann factors $\exp(-\beta M)$), the low temperature thermal excitations are completely dominated by the almost massless pions. To obtain the effects of pions in our results, we should integrate over the meson fields in the path integral formalism, which is however beyond the scope of this paper.

Even with the above-mentioned limitations, the scaled NJL models have important new features: some gluonic effects are included through the gluon condensate χ which couples the up and strange quark condensates. Thanks to this coupling, our model allows simultaneous transitions for the up and strange sectors (strong coupling), even though they tend to remain uncoupled for high chemical potentials. The coupling then allows first order transitions as a function of temperature while, within a pure NJL, they are always of the second order* (*e.g.* [8, 79]).

*The pure NJL model does, however, allow first order transitions w.r.t. density, *e.g.* [7].

C. Comparison with Lattice QCD. To make a comparison with lattice QCD*, it can be advantageous to normalize P, ε, Ts and the interaction measure $(\varepsilon - 3P)$ to T^4. The interaction measure gives the nonperturbative contribution to the thermodynamics: it vanishes in the Stefan–Boltzmann limit. It is also interesting to plot $3P$ and ε in the same picture to see how sharp is the increase of the corresponding thermodynamical function. The origin of the coefficient 3 in front of P compared to ε comes from the coincidence of their respective asymptotic T^4 behavior (see the comparison between Eq. (40) and Eq. (44)). In the same spirit, one can normalize the entropy density by a factor $3/4$ (see Eq. (47)). In this way, $3P$, ε and $3sT/4$ have the same asymptotic value $7N_c\pi^2/20$, which is a direct consequence of the number of d.o.f. which enters the model. Note that the quantities we examine are relative to the quarks. In our simplified model, the glueball only enters through the bag constant.

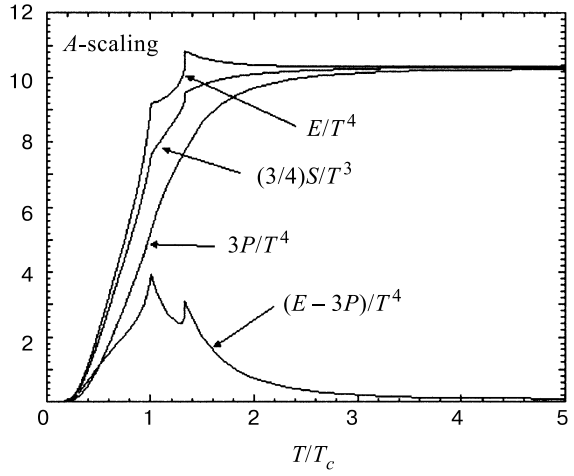

Fig. 9. Pressure, energy density, entropy density and interaction measure for a set of parameters (51,52) $M_u^0 = 300$ MeV *(a)*; for $\chi_0 = 80$ MeV

In Fig. 9 we show both the pressure and the energy and entropy densities of the A-scaling NJL model versus T/T_c ($T_c = 150$ MeV) for the set of parameters (51) ($M_u^0 = 300$ MeV, $\chi_0 = 80$ MeV), with $m_u = 0$. Here, we have taken the critical temperature corresponding to the chiral symmetry restoration connected to the up quarks.

*Because lattice QCD has only turned recently towards finite density, see *e.g.* [80], we restrict ourselves to $\mu_u = \mu_s = 0$.

Several interesting points have to be mentioned. One expects from lattice studies, *e.g.*, [39,40,45], that the thermodynamical quantities are almost vanishing below T_c, then increasing. This increase is very sharp for ε and Ts, while the pressure approaches the Stefan–Boltzmann limit very slowly. Lattice calculations show also that ε/T^4 has a peak* just above T_c, then approaching its asymptotic value from above. Finally, they also show that $\varepsilon - 3P \neq 0$ above T_c. Our results, summarized in Fig. 9, show that the model is in qualitative agreement with lattice results. The quantitative difference can be understood in the following way: lattice calculations show a rapid variation of the entropy density in a narrow region of T (≈ 10 MeV), which is traced back to the liberation of quarks and gluons. It seems then quite trivial to relate this fast increase to the confinement-deconfinement properties, which are not included in our model. This is clearly seen in the entropy density calculated with our model where the entropy is already increasing (although not as fast as near T_c) for T as low as $0.2T_c$. Once this entropy curve is understood, the general behavior of P and ε can also be deduced, see, *e.g.*, [81]. It is explicitly shown in that reference that, starting with a sharp entropy density, the energy density has a peak, and that the pressure increase above T_c is low. In fact, would the entropy be approximated by a step, we should have the exact result

$$\frac{P(T)}{P_{SB}(T)} \sim 1 - \left(\frac{T_c}{T}\right)^4, \tag{65}$$

which gives $P/P_{SB} = 50\%$ (90%) for $T/T_c = 1.2$ (1.8), independently of the details of the model. Since we are far from a step for the entropy, P/T^4 has an even weaker T dependence. This is shown in the general model for the entropy [81] and is confirmed by our particular model. On the same ground, it can also be shown that the interaction measure $(\varepsilon - 3P)/T^4$, given in Eq. (37), has a peak above T_c.

We have seen that the general behavior can be understood from the analysis of [81] which, together with the lack of confinement of our model, explains the quantitative disagreement between lattice gauge calculations and scaled NJL ones. However, our figure shows nice features not discussed extensively in the literature. If we concentrate on the energy density, it is clear that the peak has its slope broken in two places. These broken slope points coincide with the temperature where the chiral symmetry is restored. Since the current up quark mass is zero, the transition corresponding to the up quarks has no tail (see Fig. 4), leading to the first slope discontinuity while, because the transition of the strange quarks is of first order, there is in fact a jump in the energy density. Since this jump is small, it looks like a discontinuous slope. To get a nice peak, one then has to

*This is not the case for a pure gauge theory.

consider only crossovers (second order transition with nonvanishing current quark masses). Note also that a gap in energy only transforms into a change of slope for the pressure, while a change of slope in the energy plot is almost invisible in the pressure. It is evident that the energy density is the adequate quantity to be investigated in order to have insights on the order of the transition, and for extracting the critical temperature*.

Figure 10 illustrates that the broken peak of Figure 9 is due to the combined effect of a second order phase transition for the up quarks (in the chiral limit $m_u = 0$) and a weak first order transition for the strange quarks. We have taken the set of parameters ($M_u^0 = M_s^0 = 400$ MeV, $\chi_0 = 350$ MeV). In that case, there is only one critical temperature, and the transition is of second order, with the critical temperature given precisely by Eq. (53).

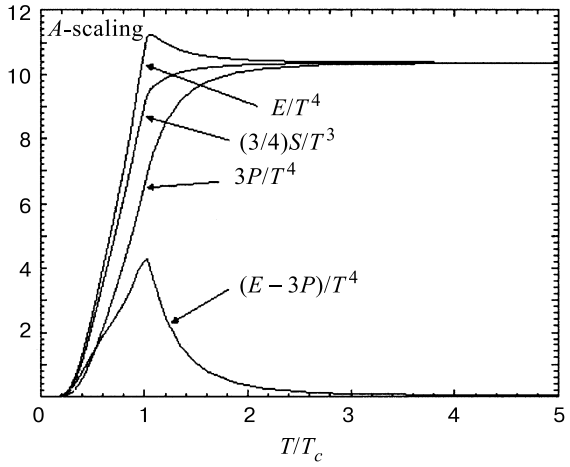

Fig. 10. Pressure, energy density, entropy density and interaction measure for a set of parameters (51,52) $M_u^0 = M_s^0 = 400$ MeV *(a)*; for $\chi_0 = 350$ MeV

All we have said for the energy density remains valid for the interaction measure (two peaks in Fig. 9 which, with $m_u \neq 0$ and a second order transition for the strange quarks, would lead to a single peak). This gives, in the limit of three degenerate flavors, the interaction measure of Fig. 10. Note that, in the chiral limit, the interaction measure just gives $4B/T^4$ (for $T \geq T_c$), B being the bag constant, see Eq. (37).

*This information can of course be obtained from the reconstruction of the quark condensates.

4. CONCLUSIONS

In this contribution, we have introduced a modified version of the Nambu–Jona-Lasinio model which takes into account the axial and scale anomalies of QCD. The model is not renormalizable, nor has it the confinement property. However, it has the dynamical breaking of chiral symmetry included and we have worked with the hypothesis that its restoration at high temperature and density is equivalent to studying the confinement-deconfinement phase transition.

We have mainly focused on analytical results for thermodynamical functions and have shown that working with different flavors introduce typical behavior for these functions.

ACKNOWLEDGMENTS

I wish to thank J. Cugnon, M. Jaminon, and Yu. L. Kalinovsky for friendly and critical discussions concerning parts of the material included here.

I wish also to thank the organizers and participants of the «Deconfinement at Finite Temperature and Density» Workshop, Dubna (Russia), October 1997 for the nice working atmosphere during the whole duration of the workshop. Most of all, I am indebted to L. Kalinovskaya for having made it running smoothly, and the Heisenberg–Landau program of the BMBF for having made it possible.

I am very grateful to V. Makoveeva and V. Makoveev for logistic support in Dubna. This work has been completed with the support of the Institut Interuniversitaire des Sciences Nucléaires de Belgique.

Appendix A
HIGH AND LOW TEMPERATURE EXPANSION OF THERMODYNAMICAL FUNCTIONS

1. Pressure. For a vanishing chemical potential, Eq. (35) reads

$$P_{\text{ideal gas}} = 2\frac{N_c}{3\pi^2}\left\{2\int_0^\infty \frac{k^4}{E_u}\frac{1}{1+e^{\beta E_u}}dk + \int_0^\infty \frac{k^4}{E_s}\frac{1}{1+e^{\beta E_s}}dk\right\}. \tag{A1}$$

Only one of these terms has to be analyzed. We define

$$P_{\text{ideal gas}}(s) = \frac{2N_c}{3\pi^2}M_s^4 \lim_{\varepsilon\to 0}\int_1^\infty \frac{\left(y^2-1\right)^{3/2}}{1+e^{\varepsilon}e^{M_s\beta y}}dy, \tag{A2}$$

where the infinitesimal quantity ε will allow one to regularize the summation that will be encountered in the following. Expanding, we get

$$P_{\text{ideal gas}}(s) = \frac{2N_c}{3\pi^2} M_s^4 \lim_{\varepsilon \to 0} \sum_{n=1}^{\infty} (-1)^{n+1} e^{-n\varepsilon} \int_1^{\infty} \left(y^2 - 1\right)^{3/2} e^{-nM_s \beta y} dy, \tag{A3}$$

which can be expressed in terms of the modified Bessel function of order two [82]

$$P_{\text{ideal gas}}(s) = \frac{2N_c}{\pi^2} M_s^4 \lim_{\varepsilon \to 0} \sum_{n=1}^{\infty} (-1)^{n+1} e^{-n\varepsilon} \frac{K_2\left(nM_s\beta\right)}{n^2 M_s^2 \beta^2}. \tag{A4}$$

This series has also been investigated in [29]. Because of the fast decrease due to the $1/n^2$ factor and because of the asymptotic behavior of K_2, it can be numerically more advantageous to use (A4) than (A3).

a. High Temperature Zero Density Expansion. The converging factor ε in (A3) and (A4) is necessary to obtain nondiverging quantities in the high temperature expansion. In such an expansion, only the first two terms are finite. Following [82],

$$K_2(z) = 2z^{-2}\left(1 - \frac{z^2}{4}\right) + \frac{1}{8} z^2 \sum_{k=0}^{\infty} \frac{\psi(k+1) + \psi(k+3)}{k!\,(2+k)!} \left(\frac{z^2}{4}\right)^k - \ln\frac{z}{2} I_2(z), \tag{A5}$$

where ψ is the Digamma function (defined as $d\ln\Gamma(z)/dz$ with $\Gamma(z)$ the Euler Gamma function) [82],

$$\psi(n+1) = -\gamma + \sum_{k=1}^{n} \frac{1}{k}, \quad \text{with} \quad \psi(1) = -\gamma, \tag{A6}$$

and where $I_2(z)$ is the other modified Bessel function of order two [82]

$$I_2(z) = \frac{z^2}{4} \sum_{k=0}^{\infty} \frac{1}{k!\,(k+2)!} \left(\frac{z^2}{4}\right)^k. \tag{A7}$$

In (A6), γ is the Euler constant.

The logarithm $\ln(z)$ in $K_2(z)$ implies a singularity at the origin. There is no Taylor expansion around it. This problem, and the way to circumvent it through the converging factor, has been established in [62] for a fermionic gas (only the first few terms of the expansion are given) and in [64–66] for a bosonic case where a full expansion, valid also at nonzero density, has been given.

Combining (A5) and (A7), we obtain

$$\left(\frac{2}{z^2}\right)\left(1-\frac{z^2}{4}\right)+\left(\frac{z^2}{4}\right)\sum_{k=0}^{\infty}\frac{1}{k!(k+2)!}\left(\frac{z^2}{4}\right)^k\times$$

$$\times\left[\frac{1}{2}\left(\psi(k+1)+\psi(k+3)\right)-\ln\left(\frac{z}{2}\right)\right]. \tag{A8}$$

This leads to

$$P_{\text{ideal gas}}(s)=\frac{2N_c}{\pi^2}M_s^4\lim_{\varepsilon\to 0}\left\{\sum_{n=1}^{\infty}(-1)^{n+1}\frac{1}{(nM_s\beta)^2}\left(\frac{2}{(nM_s\beta)^2}-\frac{1}{2}\right)+\right.$$

$$+\frac{1}{4}\sum_{n=1}^{\infty}\sum_{k=0}^{\infty}(-1)^{n+1}e^{-n\varepsilon}\frac{1}{k!(k+2)!}\left(\frac{(nM_s\beta)^2}{4}\right)^k\times$$

$$\left.\times\left[\frac{1}{2}\left(\psi(k+1)+\psi(k+3)\right)-\ln\left(\frac{(nM_s\beta)}{2}\right)\right]\right\}. \tag{A9}$$

The first two terms are easy to determine and coincide with the two nondiverging terms from the Taylor expansion around $M_s=0$. They give

$$\frac{2N_c}{\pi^2}M_s^4\left\{\frac{2}{M_s^4\beta^4}\sum_{n=1}^{\infty}(-1)^{n+1}\frac{1}{n^4}-\frac{1}{2M_s^4\beta^2}\sum_{n=1}^{\infty}(-1)^{n+1}\frac{1}{n^2}\right\}. \tag{A10}$$

They are tabulated in [82] and can be expressed through the use of the Riemann zeta function*

$$\zeta(z)=\frac{1}{1-2^{1-z}}\sum_{n=1}^{\infty}\frac{(-1)^{n+1}}{n^z}\ , \qquad \mathrm{Re}(z)>0 \tag{A11}$$

$$\zeta(-2m)=0,\ m\text{=1,2,...}, \tag{A12}$$

$$\zeta(2m)=\frac{2^{2m-1}\pi^{2m}|B_{2m}|}{(2m!)},\ \text{with } m\text{=1,2,... and } B \text{ the Bernoulli numbers,} \tag{A13}$$

*For $\mathrm{Re}(z)\leq 0$ which we shall need in the following, a converging factor $e^{-n\varepsilon}$ is needed.

which leads to

$$\frac{7}{180}N_c\pi^2T^4 - \frac{N_c}{12}M_s^2T^2. \tag{A14}$$

The contribution of the term $k = 0$ is rewritten in the form

$$\frac{2N_c}{4\pi^2}M_s^4\Bigg\{\lim_{\varepsilon\to 0}\frac{1}{2}\Bigg[\sum_{n=1}^{\infty}(-1)^{n+1}e^{-n\varepsilon}\Big(\frac{1}{2}(\psi(1)+\psi(3)) - \ln(\frac{M_s\beta}{2})\Big) -$$

$$-\sum_{n=1}^{\infty}(-1)^{n+1}e^{-n\varepsilon}\ln n\Bigg]\Bigg\}. \tag{A15}$$

Using

$$\lim_{\varepsilon\to 0}\sum_{n=1}^{\infty}(-1)^{n+1}e^{-n\varepsilon}n^z = (1-2^{1+z})\zeta(-z), \tag{A16}$$

we have

$$\frac{d}{dz}\sum_{n=1}^{\infty}(-1)^{n+1}e^{-n\varepsilon}n^z = \sum_{n=1}^{\infty}(-1)^{n+1}e^{-n\varepsilon}n^z\ln n \equiv \frac{d}{dz}\left((1-2^{1+z})\zeta(-z)\right), \tag{A17}$$

which leads to

$$\sum_{n=1}^{\infty}(-1)^{n+1}e^{-n\varepsilon}n^z\ln n = -(\ln 2)2^{1+z}\zeta(-z) - (1-2^{1+z})\zeta'(-z), \tag{A18}$$

where $\zeta'(-z) \equiv \frac{d}{dz}\zeta(z)\big\}_{-z}$.

$\zeta(0)$ is obtained from

$$-\sum_{n=1}^{\infty}(-1)^{n+1}e^{-n\varepsilon} = -\frac{e^{-n\varepsilon}}{1+e^{-n\varepsilon}} = -\frac{1}{2} \text{ when } \varepsilon\to 0, \tag{A19}$$

while $\zeta'(0)$ is given in [82]

$$\zeta'(0) = -\frac{1}{2}\ln 2\pi. \tag{A20}$$

With (A19) and (A20), (A15) gives

$$\frac{2N_c}{4\pi^2}M_s^4\frac{1}{2}\Bigg\{\frac{1}{2}\cdot\frac{1}{2}\left(\psi(1)+\psi(3)-2\ln(\frac{M_s\beta}{2})\right) - \frac{1}{2}\ln\left(\frac{2}{\pi}\right)\Bigg\}. \tag{A21}$$

We still need the $k > 0$ terms of the expansion. With (A16) and (A18), they are

$$\frac{2N_c}{4\pi^2}M_s^4 \lim_{\varepsilon\to 0}\left\{\sum_{k=1}^{\infty}\frac{(M_s\beta)^{2k}}{k!(k+2)!4^k}\left[\frac{1}{2}\left(\psi(k+1)+\psi(k+3)-2\ln\left(\frac{M_s\beta}{2}\right)\right)\times\right.\right.$$

$$\left.\left.\times(1-2^{1+2k})\zeta(-2k)+(\ln 2)2^{1+2k}\zeta(-2k)+(1-2^{1+2k})\zeta'(-2k)\right]\right\}. \quad \text{(A22)}$$

Equation (A6) implies

$$\begin{aligned}\psi(1) &= -\gamma, \\ \psi(3) &= -\gamma+\frac{3}{2},\end{aligned} \quad \text{(A23)}$$

so that (A12), (A14), (A21), (A22) lead to

$$\begin{aligned}P_{\text{ideal gas}}(s) = \frac{7}{180}N_c\pi^2T^4 - \frac{N_c}{12}M_s^2T^2 + \\ +\frac{N_c}{16\pi^2}M_s^4\left(-2\gamma+\frac{3}{2}\right) - \frac{N_c}{8\pi^2}M_s^4\ln\left(\frac{M_s\beta}{\pi}\right) + \\ +\frac{N_c}{2\pi^2}M_s^4\sum_{k=1}^{\infty}\frac{(M_s\beta)^{2k}}{k!(k+2)!4^k}(1-2^{1+2k})\zeta'(-2k).\end{aligned} \quad \text{(A24)}$$

It is clear that the converging factor has regularized the summation* of the expansion. Note from (A24) that the separation into a logarithmic term and a constant one is arbitrary: one can always write $\ln(aM_s\beta) = \ln(M_s\beta) + \ln a$ (a being a dimensionless constant) and put $\ln a$ into the constant term. This has some importance for the interpretation of the high temperature results.

To write (A24) into a form involving only elementary functions, we still need to know $\zeta'(-2k)(k \geq 1)$, *i.e.*,

$$-\frac{1}{(1-2^{1+2k})}\sum_{n=1}^{\infty}(-1)^{n+1}e^{-n\varepsilon}n^{2k}\ln n, \quad \text{(A25)}$$

because of (A18) and (A12). Using [82]

$$2^{1-z}\Gamma(z)\zeta(z)\cos\left(\frac{\pi z}{2}\right) = \pi^z\zeta(1-z) \quad \text{(A26)}$$

*Summations of this kind are called Euler sums [83].

and

$$\Gamma(z)\Gamma(1-z) = \frac{\pi}{\sin(\pi z)}, \tag{A27}$$

we have

$$2^{1-z}\frac{\pi}{\sin(\pi z)}\zeta(z)\cos\left(\frac{\pi z}{2}\right) = \pi^z\Gamma(1-z)\zeta(1-z), \tag{A28}$$

so that

$$\lim_{z\to -2k}\frac{\pi}{\sin(\pi z)}\zeta(z) = (-1)^k 2^{-2k-1}\pi^{-2k}\Gamma(1+2k)\zeta(1+2k). \tag{A29}$$

With

$$\lim_{z\to -2k}\frac{\pi}{\sin(\pi z)}\zeta(z) = \frac{0}{0} = \frac{\pi\zeta'(-2k)}{\pi\cos(-2\pi k)} = \zeta'(-2k), \tag{A30}$$

we finally obtain

$$\zeta'(-2k) = \frac{1}{2}(-1)^k(2\pi)^{-2k}\Gamma(1+2k)\zeta(1+2k). \tag{A31}$$

Equation (A24) is then rewritten into the form

$$P_{\text{ideal gas}}(s) = \frac{7}{180}N_c\pi^2T^4 - \frac{N_c}{12}M_s^2T^2 +$$
$$+\frac{N_c}{16\pi^2}M_s^4\left(-2\gamma+\frac{3}{2}\right) - \frac{N_c}{8\pi^2}M_s^4\ln\left(\frac{M_s\beta}{\pi}\right) +$$
$$+\frac{N_c}{2\pi^2}M_s^4\sum_{k=1}^{\infty}\frac{(M_s\beta)^{2k}}{k!(k+2)!4^k}(1-2^{1+2k})\frac{1}{2}(-1)^k(2\pi)^{-2k}\Gamma(1+2k)\zeta(1+2k), \tag{A32}$$

which only necessitates the evaluation of known functions.

b. Low Temperature Zero Density Expansion. We can search for a low temperature expansion, $\beta\to\infty$, starting from (A1) or (A4). The last one is better suited because of the well known asymptotic expansion of K_2 [84]

$$K_i(z) \approx \sqrt{\frac{\pi}{2z}}e^{-z}\Big\{1+\frac{4i^2-1}{8z}+\frac{(4i^2-1)(4i^2-9)}{2!(8z)^2}+$$
$$+\frac{(4i^2-1)(4i^2-9)(4i^2-25)}{3!(8z)^3}+\ldots\Big\}. \tag{A33}$$

Combining (A4) and (A33), we have

$$P_{\text{ideal gas}}(s) \approx \frac{2N_c}{\pi^2} M_s^4 \sum_{n=1}^{\infty} \frac{(-1)^{n+1}}{n^2 M_s^2 \beta^2} \sqrt{\frac{\pi}{2nM_s\beta}} e^{-nM_s\beta} \times \left\{ 1 + \frac{15}{8nM_s\beta} + \frac{15 \cdot 7}{2!(8nM_s\beta)^2} + \frac{15 \cdot 7 \cdot (-9)}{3!(8nM_s\beta)^3} + ... \right\}. \quad \text{(A34)}$$

When β is large, we are in the chirally broken phase where the quark masses are the constituent masses. Since the expanding parameter is βM_i, $i = u, s$, the approximation (A34) becomes better as βM_i is increased. In Section 3, it is shown that the mass variation is low for $T \lesssim 100$ MeV. For a constituent quark mass of about 400 MeV (at $T = 0$) βM_i is, at least, 4. The expansion (A34) is then perfectly justified. In that case, the first term $n = 1$ is enough and the pressure is

$$P_{\text{ideal gas}}(s) \approx \frac{4N_c \beta^{-5/2}}{(2\pi)^{3/2}} M_s^{3/2} e^{-M_s\beta} \times \left\{ 1 + \frac{15}{8M_s\beta} + \frac{15 \cdot 7}{2!(8M_s\beta)^2} + \frac{15 \cdot 7 \cdot (-9)}{3!(8M_s\beta)^3} + ... \right\}. \quad \text{(A35)}$$

We have checked that for the set of parameters $(M_u^0 = 300, \chi_0 = 80)$ MeV (see Section 3) this expansion is not well suited. In that case, the second term $n = 2$ in (A34), as well as the three corrections to «1» for both $n = 1$ and $n = 2$, are necessary to reproduce results valid up to 100 MeV.

c. Finite Density, Zero Temperature. For finite density at vanishing temperature, Eq. (35) can be exactly integrated. We have $n_{i+} = 0$, $n_{i-} = \theta(\mu_i - E_i)$ and $\mu_i = \sqrt{k_{F_i}^2 + M_i^2}$, where k_{F_i} is the Fermi momentum of the ith flavor, so that

$$P_{\text{ideal gas}}(s) = \frac{N_c}{3\pi^2} \int_0^{k_{F_s}} dk \; \frac{k^4}{E_s}, =$$

$$= \frac{N_c}{3\pi^2} \left\{ k_{F_s}^3 \mu_s - 3 \Big[\frac{k_{F_s}}{4} \mu_s^3 - \frac{M_s^2}{8} k_{F_s} \mu_s - \frac{M_s^4}{8} \ln \left(\frac{k_{F_s} + \mu_s}{M_s} \right) \Big] \right\}. \quad \text{(A36)}$$

2. Energy Density. *a. High Temperature Zero Density Expansion.* The combining of Eqs. (43), (A32) immediately gives

$$\varepsilon_{\text{ideal gas}}(s) = \frac{7}{60} N_c \pi^2 T^4 - \frac{N_c}{12} M_s^2 T^2 + \frac{N_c}{16\pi^2} M_s^4 \left(2\gamma + \frac{1}{2} \right) + \frac{N_c}{8\pi^2} M_s^4 \ln \left(\frac{M_s \beta}{\pi} \right) -$$

$$-\frac{N_c}{2\pi^2}M_s^4\sum_{k=1}^{\infty}\frac{(M_s\beta)^{2k}}{k!(k+2)!4^k}(2k+1)(1-2^{1+2k})\times$$

$$\times\frac{1}{2}(-1)^k(2\pi)^{-2k}\Gamma(1+2k)\zeta(1+2k). \tag{A37}$$

b. Low Temperature Zero Density Expansion. Equation (43) is not well-suited because it would imply taking the derivative of a truncated series (see Eq. (A34)). It is better to search for the expansion of the exact solution in terms of the modified Bessel function obtained in [50]

$$\varepsilon_{\text{ideal gas}}(s)=3P_{\text{ideal gas}}(s)+\frac{2N_c}{\pi^2}M_s^4\sum_{n=1}^{\infty}(-1)^{n+1}\frac{K_1(nM_s\beta)}{nM_s\beta}. \tag{A38}$$

Its low temperature asymptotic expansion is obtained from Eq. (A34) for the first term and from Eq. (A33) with $i=1$ [84] for the second one. We then have

$$\begin{aligned}\varepsilon_{\text{ideal gas}}(s)\approx{}&3\frac{2N_c}{\pi^2}M_s^4\sum_{n=1}^{\infty}\frac{(-1)^{n+1}}{n^2M_s^2\beta^2}\sqrt{\frac{\pi}{2nM_s\beta}}e^{-nM_s\beta}\\&\times\left\{1+\frac{15}{8nM_s\beta}+\frac{15\cdot7}{2!(8nM_s\beta)^2}+\frac{15\cdot7\cdot(-9)}{3!(8nM_s\beta)^3}+...\right\}\\&+\frac{2N_c}{\pi^2}M_s^4\sum_{n=1}^{\infty}(-1)^{n+1}\frac{1}{nM_s\beta}\sqrt{\frac{\pi}{2nM_s\beta}}e^{-nM_s\beta}\\&\times\left\{1+\frac{3}{8nM_s\beta}+\frac{3\cdot(-5)}{2!(8nM_s\beta)^2}+\frac{3\cdot(-5)\cdot(-21)}{3!(8nM_s\beta)^3}+...\right\}.\end{aligned} \tag{A39}$$

Once again we can limit ourselves to $n=1$ or $n=1,2$, depending upon the chosen set of parameters (M_u^0,χ_0). However the first two or three corrections to «1» are necessary.

c. Finite Density, Zero Temperature. As for the pressure, Eq. (36) can be exactly integrated. It is however more judicious to use the vanishing nature of the entropy at $T=0$ in order to get (Eq. (34)),

$$\varepsilon_{\text{ideal gas}}=-P_{\text{ideal gas}}+\mu_i\rho_i, \tag{A40}$$

where ρ_i is given by Eq. (27), *i.e.*,

$$\lim_{T\to0}\rho_i=\frac{N_c}{3\pi^2}k_{F_i}^3. \tag{A41}$$

Using (A36), (A40) and (A41), we obtain

$$\varepsilon_{\text{ideal gas}}(s)=\frac{N_c}{\pi^2}\Big[\frac{k_{F_s}}{4}\mu_s^3-\frac{M_s^2}{8}k_{F_s}\mu_s-\frac{M_s^4}{8}\ln\left(\frac{k_{F_s}+\mu_s}{M_s}\right)\Big]. \tag{A42}$$

3. Entropy Density. *a. High Temperature Zero Density Expansion.* The use of Eqs. (46), (A32) gives

$$s(s) = \frac{7}{45}N_c\pi^2T^3 - \frac{N_c}{6}M_s^2T + \frac{N_c}{8\pi^2}M_s^4\beta -$$

$$-\frac{N_c}{2\pi^2}M_s^4\beta\sum_{k=1}^{\infty}\frac{(M_s\beta)^{2k}}{k!(k+2)!4^k}2k(1-2^{1+2k})\times$$

$$\times\frac{1}{2}(-1)^k(2\pi)^{-2k}\Gamma(1+2k)\zeta(1+2k). \tag{A43}$$

b. Low Temperature Zero Density Expansion. We can obtain this expansion starting from Eq. (34) with $\mu_i = 0$:

$$s(s) = \beta(P_{\text{ideal gas}}(s) + \varepsilon_{\text{ideal gas}}(s)), \tag{A44}$$

so that, using Eqs. (A34), (A39), we have

$$s(s) \approx 4\beta\frac{2N_c}{\pi^2}M_s^4\sum_{n=1}^{\infty}\frac{(-1)^{n+1}}{n^2M_s^2\beta^2}\sqrt{\frac{\pi}{2nM_s\beta}}e^{-nM_s\beta}\times$$

$$\times\left\{1+\frac{15}{8nM_s\beta}+\frac{15\cdot7}{2!(8nM_s\beta)^2}+\frac{15\cdot7\cdot(-9)}{3!(8nM_s\beta)^3}+...\right\}+$$

$$+\frac{2N_c}{\pi^2}M_s^4\beta\sum_{n=1}^{\infty}(-1)^{n+1}\frac{1}{nM_s\beta}\sqrt{\frac{\pi}{2nM_s\beta}}e^{-nM_s\beta}\times$$

$$\times\left\{1+\frac{3}{8nM_s\beta}+\frac{3\cdot(-5)}{2!(8nM_s\beta)^2}+\frac{3\cdot(-5)\cdot(-21)}{3!(8nM_s\beta)^3}+...\right\}. \tag{A45}$$

Once again we can limit ourselves to $n = 1$ or $n = 1, 2$, depending upon the chosen set of parameters (M_u^0, χ_0). However the first two or three corrections to «1» are necessary.

c. Finite Density, Zero Temperature. It is clear that

$$s(s) = 0, \tag{A46}$$

in agreement with the third principle of thermodynamics.

REFERENCES

1. **Cheng T.P., Li L.F.** — Gauge Theory of Elementary Particle Physics, Clarendon Press, Oxford, 1984.
2. **Nambu Y., Jona-Lasinio G.** — Phys. Rev., 1961, v.122, p.345.
3. **Nambu Y., Jona-Lasinio G.** — Phys. Rev., 1961, v.124, p.246.
4. **Volkov M.K.** — Ann. Phys., 1984, v.157, p.282.
5. **Van den Bossche B.** — A Chiral Quark Model with Three Flavors and Anomalies, In preparation, a preliminary version can be found on nucl-th/9807010, 1998.
6. **Ripka G.** — Quarks Bound by Chiral Fields: the Quark Structure of the Vacuum and of Light Mesons and Baryons, Oxford Studies in Nuclear Physics, Oxford University Press, 1997.
7. **Klevansky S.P.** — Rev. Mod. Phys., 1992, v.64, p.649.
8. **Hatsuda T., Kunihiro T.** — Phys. Rep., 1994, v.247, p.221.
9. **Alkofer R., Reinhardt H., Weigel H.** — Phys. Rep., 1996, v.265, p.139.
10. **Meissner Th. et al.** — Baryons in Effective Chiral Quark Models with Polarized Dirac Sea, Bochum Preprint RUB-TPH-42/93 – hep-ph/9401216, 1994.
11. **Bijnens J.** — Phys. Rep., 1996, v.265, p.369.
12. **Alkofer R., Reinhardt H.** — Chiral Quark Dynamics, Lecture Notes in Physics, New Series m: Monographs, Springer-Verlag Berlin Heidelberg, 1995.
13. **Ebert D., Reinhardt H., Volkov M.K.** — In: Progress in Particle and Nuclear Physics, A. Fäßler, ed., v.33, p.1. Pergamon Press, Oxford, 1994.
14. **Vogl U., Weise W.** — In: Progress in Particle and Nuclear Physics, A. Fäßler, ed., v.27, p.195. Pergamon Press, Oxford, 1991.
15. **Weise W.** — Hadrons in the NJL Model. In: Lecture presented at the Center for Theoretical Physics, Seoul National University, Seoul, Korea, Sept. 1992.
16. **Ebert D., Kalinovsky Y.L., Volkov M. K.** — Phys. Lett., 1993, v.B301, p.231.
17. **Kusaka K., Volkov M.K., Weise W.** — Phys. Lett., 1993, v.B302, p.145.
18. **Kalinovsky Y.L., Volkov M. K.** — Mod. Phys. Lett., 1994, v.A9, p.993.
19. **Donoghue J.F., Golowich E., Holstein B.R.** — Dynamics of the Standard Model, Cambridge Monographs on Particle Physics, Nuclear Physics and Cosmology, Cambridge University Press, 1992.
20. **Veneziano G.** — Nucl. Phys., 1979, v.B159, p.213.
21. **Witten E.** — Nucl. Phys., 1979, v.B156, p.269.
22. **'t Hooft, G.** — Phys. Rep., 1986, v.142, p.357.
23. **Witten E.** — Ann. Phys., 1980, v.128, p.363.
24. **Di Vecchia P., Veneziano G.** — Nucl. Phys., 1980, v.B171, p.253.
25. **Rosenzweig C., Schechter J., Trahern C.G.** — Phys. Rev., 1980, v.D21, p.3388.
26. **Schechter J.** — Phys. Rev., 1980, v.D21, p.3393.
27. **Kleinert H.** — In: Understanding the Fundamental Constituents of Matter, A.Zichichi, ed., p.289, Plenum Press, New York, International School of Subnuclear Physics, Erice, Italy, 1976.
28. **Kleinert H** — Fortschr. Phys., 1978, v.6, p.565.
29. **Jaminon M., Van den Bossche B.** — Nucl. Phys., 1994, v.A567, p.865.

30. **Jaminon M., Van den Bossche B.** — Nucl. Phys., 1995, v.A582, p.517.
31. **Jaminon M., Van den Bossche B.** — Z. Phys., 1994, v.C64, p.339.
32. **Gomm H. et al.** — Phys. Rev., 1986, v.D33, p.801.
33. **Jain P., Johnson R., Schechter J.** — Phys. Rev., 1988, v.D38, p.1571.
34. **Van den Bossche B.** — Ph.D. thesis, Université de Liège, 1996.
35. **Roberts C.D., Williams A.G., Krein G.** — Int. J. Mod. Phys., 1992, v.A7, p.5607.
36. **Campbell B.A., Ellis J., Olive K.A.** — Phys. Lett., 1990, v.B235, p.325.
37. **Campbell B.A., Ellis J., Olive K.A.** — Nucl. Phys., 1990, v.B345, p.57.
38. **Jaminon M., Ripka G.** — Ann. Phys., 1992, v.218, p.51.
39. **Laermann E.** — Nucl. Phys., 1996, v.A610, p.1.
40. **Karsch F.** — Nucl. Phys., 1995, v.A590, p.367c.
41. **Iwassaki Y. et al.** — Z. Phys., 1996, v.C71, p.343.
42. **Brown F.R. et al.** — Phys. Rev. Lett., 1990, v.65, p.2491.
43. **Schäfer T.** — Nucl. Phys., 1996, v.A610, p.13.
44. **DeTar C.** — Quark Gluon Plasma in Numerical Simulations of Lattice QCD, hep-ph/9504325, 1995.
45. LATTICE 96, XIV International Symposium on Lattice Filed Theory, Nucl. Phys., v.B53 (Proc. Suppl.), 1997.
46. **Kogut J.B., Sinclair D.K., Wang K.C.** — Phys. Lett., 1991, v.B263, p.101.
47. **Koch V., Brown G.E.** — Nucl. Phys., 1993, v.A560, p.345.
48. **Bender A. et al.** — Phys. Rev. Lett., 1996, v.77, p.3724.
49. **Brown G.E. et al.** — Nucl. Phys., 1993, v.A560, p.1035.
50. **Cugnon J., Jaminon M., Van den Bossche B.** — Nucl. Phys., 1996, v.A598, p.515.
51. **Schmidt S.** — Ph.D. thesis, Universität Rostock, 1995.
52. **Blaschke D. et al.** — Nucl. Phys., 1995, v.A586, p.711.
53. **Hüfner J. et al.** — Ann. Phys., 1994, v.234, p.225.
54. **Zhuang P., Hüfner J., Klevansky S.P.** — Nucl. Phys., 1994, v.A576, p.525.
55. **Zhuang P.** — Phys. Rev., 1995, v.C50, p.2256.
56. **Nikolov E.N. et al.** — Nucl. Phys., 1996, v.A608, p.411.
57. **Carter G.W., Ellis P.J., Rudaz S.** — Nucl. Phys., 1998, v.A628, p.325.
58. **Diu B. et al.** — Élements de physique statistique, Enseignement des sciences, Hermann, 1989.
59. **Fetter A.L., Walecka J.D.** — Quantum Theory of Many-Particle Systems, McGraw-Hill, 1971.
60. **Asakawa M., Yazaki K.** — Nucl. Phys., 1989, v.A504, p.668.
61. **Adami C., Brown G.E.** — Phys. Rep., 1993, v.234, p.1.
62. **Dolan L., Jackiw R.** — Phys. Rev., 1974, v.D9, p.3320.
63. **Kapusta J.I.** — Finite-Temperature Field Theory, Cambridge monographs on mathematical physics, Cambridge University Press, 1989.
64. **Haber H.E., Weldon H.A.** — Phys. Rev. Lett., 1981, v.23, p.1497.
65. **Haber H.E., Weldon H.A.** — Phys. Rev., 1982, v.D25, p.502.

66. **Haber H.E., Weldon H.A.** — J. Math. Phys., 1992, v.23, p.1852.

67. **Goffe W.L., Ferrier G.D., Rogers J.** — J. of Econometrics, 1994, v.60, p.65.

68. **Blaizot J.-P., Méndez-Galain R.** — Phys. Lett., 1991, v.B271, p.32.

69. **Rehberg P., Klevansky S.P., Hüfner J.** — Phys. Rev., 1996, v.C53, p.410.

70. **Lutz M., Klimt S., Weise W.** — Nucl. Phys., 1992, v.A542, p.521.

71. **Méndez-Galain R. et al.** — Europhys. Lett., 1991, v.14, p.7.

72. **Jaminon M. et al.** — Nucl. Phys., 1992, v.A537, p.418.

73. **Jaminon M., Ripka G.** — Nucl. Phys., 1993, v.A564, p.505.

74. **Blaschke D. et al.** — Phys. Rev., 1996, v.C53, p.2394.

75. **Gasser J., Leutwyler H.** — Phys. Lett., 1987, v.B184, p.83.

76. **Gasser J., Leutwyler H.** — Ann. Phys., 1984, v.158, p.142.

77. **Kusaka K., Weise W.** — Nucl. Phys., 1994, v.A580, p.383.

78. **Kusaka K., Weise W.** — Phys. Lett., 1992, v.B288, p.6.

79. **Klimt S., Lutz M., Weise W.** — Phys. Lett., 1990, v.B249, p.386.

80. **Barbour I.M., Kogut J.B., Morrison S.E.** — Nucl. Phys., 1997, v.B53 (Proc. Suppl.), p.456.

81. **Asakawa M., Hatsuda T.** — Nucl. Phys., 1996, v.A610, p.470.

82. **Gradshteyn I.S., Ryzhik I.M.** — Table of Integrals, Series and Products, Academic Press, 1965.

83. **Bender C.M., Orszag S.A.** — Advanced Mathematical Methods for Scientists and Engineers, McGraw-Hill Book Company, 1978.

84. **Abramowitz M., Stegun I.A.** — Handbook of Mathematical Functions, Dover Publications, Inc., 1970.